Indian Journal of Engineering & Materials Sciences
Vol. 32, June 2025, pp. 342-363
DOI: 10.56042/ijems.v32i03.15879

# Significance of ductility on aseismic design of flexural members for normal to high strength concrete

Bibhas Mandal[a1] & Santanu Bhanja[b]

[a]National Institute of Technology, Arunachal Pradesh, Jote, Papum Pare, Arunachal Pradesh 791 123, India

[b]National Institute of Technical Teachers' Training & Research, Kolkata (under MoE, Govt. of India), Block -FC, Sector – III, Salt Lake, West Bengal 700 106, India

*Received: 20 December 2024 ; accepted: 02 April 2025*

The standards or codes of practice of different countries set limits on the minimum and maximum longitudinal reinforcement in beams. On evaluation of the design parameters of these limiting sections, behavior of all sections in flexure can be assessed, as they will lie within the domain of these two conditions. The present study has been directed towards assessment of the behavior of flexural members up to and beyond limit states in accordance with the provision of different standards. IS:456-2000 being more than twenty-four years old seems to be outdated w.r.t the present-day material properties and design provisions whereas these have been covered in a befitting manner in IRC:112-2020 which is in line with international standards. Load based prescriptive method of design ends at design load levels and cannot provide any solution for design beyond the design loads either due to overloading or due to larger deformations which can lead to considerable damage or even actual collapse. For this the damage level of the sections at different performance-based limit states beyond the limit state of collapse need to be assessed as per the provisions of Performance Based Design (PBD). In the present work a comprehensive study on the curvature ductility and deformation levels of sections in flexure as per IRC:112-2020 have been performed and compared with the acceptance criteria as per international guidelines and standards.

**Keywords:** Ductility, Flexural member, Optimum aseismic design, Performance based design, Plastic rotation

## 1 Introduction

The present philosophy of design of RC sections as per the codes of practice generally follow the prescriptive method based on loads. For both strength and serviceability design it needs to be ensured that the specified failure criteria are not crossed under ultimate and working loads. As per the limit state method of design, serviceability conditions like deformations of a section are checked only at service loads, and it is implied that if the section is safe from service ability view point at working loads, the performance of the section at ultimate loads will not endanger its safety. In case of a seismic design, under-reinforced sections are always desirable because of higher ductility. If a designer aims at a section with minimum percentage of tension reinforcement, i.e., maximum under-reinforced section, the section might be safe from strength consideration if the external loading is low, but the amount of plastic rotations that can develop in the section in order to mobilize the huge amount of inelastic strain in the reinforcement might result in significant damage of the section[1]. The minimum and maximum amount of tension reinforcement are provided in different standards, and design should be restricted within these two critical conditions. In India design of reinforced concrete sections are performed as per the requirements of IS:456-2000[2]. Code of practice for concrete bridges IRC:112-2020 though deals with bridge design but provides philosophy and necessary guidelines for design of reinforced concrete sections[3]. This standard, being recently revised, has incorporated modern day materials, design methodology and is in line with the relevant international standards like Eurocode-2[4]. It is expected that the forthcoming revision of IS 456 will incorporate similar design provisions. IS 456 permits structural concrete up to M60 and the design parameters provided in the standard for HYSD bars are limited to Fe 500 grade steel though now-a-days higher strength of materials are being commercially used throughout the country. The design provisions which depend on the stress-strain relationship of the materials have also undergone significant modifications with respect to those prescribed in

*Corresponding author
(E-mail: bibhas.phd23@nitap.ac.in, bibhasman1996@gmail.com)

IS:456-2000[5] Though the basic design provisions for reinforced concrete sections as per the guidelines of IRC:112[3] are available, quantifications of ductility values and deformation levels are yet to be reported[6]. The present work is a humble effort to fill up this gap. IS:456-2000 deals with general requirements of plain and reinforced concrete which are applicable to all types of structures and deals with strength and serviceability requirements. IS:13920-2016[7] prescribes seismic resistant design and incorporates the requirements of ductility in design and detailing by using simple guidelines and drawings. Hence this standard can be considered as an add-on standard to IS:456 for design of seismic resistant structures[8]. In IRC112:2020 two types of bilinear stress-strain relationships for steel have been prescribed - one is with an inclined plastic branch and another with horizontal plastic branch. In the present work, the relationship with the horizontal plastic branch has been used for Fe 415 to Fe 600 HSD steel with M20 to M90 grades of concrete which are permitted by IRC:112. For singly reinforced beam sections, the two terminal conditions of design can be stated as– maximum under-reinforced section with minimum percentage of tension reinforcement and the maximum permitted section with maximum percentage of tension reinforcement. Any section designed in flexure will lie between these two limiting conditions. The section parameters for these two conditions along with those for the balanced condition have been evaluated. In the present paper strain ductility and curvature ductility values of sections have been calculated based on first principles. In performance-based design the different performance-based limit states are quantified with respect to section deformations and corresponding damage levels. Though performance-based design is yet to be codified in many of the countries, the general guidelines are almost universally accepted[9]. However, in prescriptive method of design, the design process ends when the limit states are reached and no further checking of section conditions are performed. The minimum percentage of tension reinforcements in beams are generally provided from the consideration of cracking moment of the section but are not checked with respect to damage levels corresponding to different performance-based limit states. Hence some correlation between the prescriptive method of design and PBD needs to be developed specially for sections with minimum area of tensile reinforcement and seismic conditions where over-loading beyond the design loads can be a routine phenomenon. The requirements of a seismic design should be considerably different from those of the general design provisions as per prescriptive method of design. In flexural members as the percentages of tension reinforcement is reduced that is the level of under-reinforcement is increased the associated strains in steel will also increase. However, the minimum percentage of tension reinforcement should not result in strains higher than the permitted design strain levels which is only specified stress-strain relationship of steel with inclined plastic branch. For the stress-strain relationships with horizontal plastic branch this condition need not be checked as the maximum limiting strain is not specified by the code and the strain values are open ended. With minimum percentage of tension reinforcement there is a possibility that the curvature values along with the associated plastic rotations might exceed the performance-based limit state conditions corresponding to the collapse stage of the section. In this context the present research work highlights the shortcomings of the standard with respect to the specified minimum percentage of tension reinforcement in beams. In the following paragraph an attempt has been made to highlight some of the important observations made by previous researchers working in this direction. Ductility of reinforced concrete beams is a crucial property that enables structures to effectively dissipate energy during seismic loading. As a result, the occurrence of brittle failures in RC structures can be effectively prevented[10,11]. As per IS:456-2000 and IS:13920-2016, curvature ductility and plastic rotation values for flexural members have already been published [1,7]. Arslan has suggested that in modern approaches to RC section design, stiffness is the most relevant parameter for serviceability requirements under small frequent earthquakes[12]. In medium frequent earthquakes, strength is utilized to control inelasticity. However, under large frequent earthquakes, ductility plays the main role in collapse prevention.[13] As per research by Xie *et al*. it has been reported that deformation of a section is influenced by several factors, including the amount of tension reinforcement, quantity of compression reinforcement, area of lateral ties, and strength of concrete etc.[14] Another study suggests that with a constant amount of tension reinforcement, ductility

decreases as the strength of concrete increases, and vice versa[15]. In case of seismic design, it has been reported that the curvature ductility factor of at least 10 is preferrable for any section[16]. Omar K. Alghazawi stated that curvature ductility increases as the transverse reinforcement ratio increases under static stress[17].As per another study by Mandal P. *et. al.* has inferred that there is no substantial impact onspacing of transverse reinforcement on the curvature ductility[18]. Curvature ductility of any beam section is governed by the level of the section being under-reinforced or over-reinforced, which totally depends on the percentage of compression and tension reinforcement provided and cover to the reinforcement[19]. It has been reported that for singly reinforced sections made of high strength concrete the evaluation of curvature ductility is required for calculating the ratio of maximum allowed tensile reinforcement or a maximum depth of the area of compression concrete and for normal strength concrete, the standards and methodology needed to estimate the curvature ductility, are based on the experimental findings[20]. Experiment performed by Opabola and Elwood have proved that beams exhibited significant capacity to withstand inelastic drift demands without compromising their lateral resistance with plastic rotation dominating their response[21]. As per another research work it has been stated that, once the flexural reinforcement yields, due to the plastic hinge rotation, the shear strength capacity is diminished because of the concrete's loss of shear strength[22]. The value of plastic rotation capacity increases as the ratio of $\rho'/\rho$ and the concrete compressive strength increase, where $\rho'$ and $\rho$ is the tension and compression reinforcement respectively[23]. In the present work an attempt has been made to assess the behavior of flexural members in the light of ductility and plastic rotation values which can act as very useful tool for seismic design of flexural members.IS:456 allows only design of under-reinforced and balanced RC beam sections. But as per IRC:112-2020, all types of sections i.e., under-reinforced, balanced, and over-reinforced are permitted in the design of flexural members. Design is restricted within the maximum and minimum percentage of tension reinforcement. Hence in the domain of flexural design two terminal section conditions can be considered- one with minimum percentage of tension reinforcement, and another with maximum percentage of tension reinforcement. 1

The main objective of this study is to investigate the flexural behavior of reinforced concrete sections for these terminal conditions as permitted by IRC:112. The quantification of the ductility and plastic rotation values will help in understanding the behavior of the sections along with the considerations of strength and serviceability.

The objectives of the present research work can be summarized as follows.

1) To calculate the design parameters for sections subjected to flexure using the simplified bilinear stress-strain relationship of steel and parabolic-rectangular stress-strain relationship of unconfined concrete in accordance with the reinforced concrete design provisions of IRC:112-2020.

2) To investigate the section condition with maximum percentage of tension reinforcement i.e., whether the maximum percentage is less or higher than the balanced percentage.

3) To determine strain ductility values of sections for all grades of concrete and steel permitted by IRC 112-2020.

4) To determine the values of curvature ductility and plastic rotations of three critical categories of sections i.e., sections with minimum, balanced, and maximum percentages of tension reinforcement for all grades of concrete and steel i.e., from M20 to M90 and Fe 415 to Fe 600.

5) To compare the strain/deformation values obtained in the present study with the reference values provided in the specialist literature/international standards on performance-based design and to evaluate the performance level of the sections.

Apart from strength and serviceability, in the present methodology of aseismic design, ductility plays a vital role. The properties of strength and ductility are conflicting in nature as increase in strength generally results in reduction in ductility. Hence a balance between these two considerations is necessary for optimal design. There are different types of ductility, and their definitions and implications are different. The process of evaluation of different ductility is quite complex and cumbersome as it depends on several factors like materials property, types of sections, reinforcement provided, stress-strain relationships etc. However, to predict the behavior of sections, quantifications of different types of ductility are necessary. In the present work strain ductility, curvature ductility and plastic rotations of terminal sections permitted in

flexure have been evaluated. These values can act as excellent tools for optimal design of reinforced concrete sections in flexure.

## 2 Materials and Methods

### 2.1 Discussion on design philosophy of IRC 112-2020 with respect to Eurocode-2

IRC 112:2020, which deals with the design of concrete road bridges, shares a similar design philosophy with 1st generation of Eurocode - Eurocode 1992-1-1 (2004)for design of RC sections, though there exist some notable differences especially regarding material specifications. Eurocode 2 outlines concrete design criteria based on cylindrical strengths from 12 MPa to 90 MPa along with corresponding cube strengths ranging from 15 MPa to 105 MPa. In contrast, IRC 112 considers only cube strengths between 20 MPa and 90 MPa. As per IRC 112 design strength of concrete has been prescribed as 0.446 of the concrete cube strengths($f_{ck}$), while as per Eurocode 2 this is defined by the following expression, $\alpha_{cc}\left(\frac{f_{ck}}{\gamma_c}\right)$, where $f_{ck}$ is cylindrical strength of concrete, $\alpha_{cc}$ is the non-dimensional parameter ranging between 0.8 to 1 and $\gamma_c$ is the material safety factor. The values of $\varepsilon_{c2}$ and $\varepsilon_{cu2}$ are constant up to concrete cube strength of 60MPa as per IRC 112 and up to cylindrical strength of 50 MPa as per Eurocode-2, beyond that the values are marginally different for the two standards, where $\varepsilon_{c2}$ and $\varepsilon_{cu2}$ refers to yield strain and ultimate strains in concrete respectively. These modifications in strain values will result in changes in strength and ductility design of sections. Both follows similar parabolic stress-strain relationship for unconfined concrete. Despite these distinctions, the safety factors for concrete remain the same in both standards. Steel grade specifications also differ as Eurocode 2 defines the characteristic strength of steel ($f_{yk}$) between 400 MPa to600 MPa, further categorizing it into ductility classes A, B, and C. In contrast, IRC 112 specifies steel grades—Fe415, Fe415D, Fe415S, Fe500S, Fe500, Fe550, Fe 550D, and Fe600. Both codes present two stress-strain relationships for steel: one featuring a bilinear curve with an inclined plastic branch with a maximum strain limit ($\varepsilon_{ud}$) subjected to a maximum stress of $k\left(\frac{f_{yk}}{\gamma_s}\right)$, and another exhibiting a horizontal plastic branch with no limitation in strain. For design purposes, the horizontal plastic branch is commonly used due to its simplicity in mathematical calculations.[5,6] Both standards adopt a strength design philosophy for the ultimate limit state.[9] In the present work, ductility values of singly reinforced concrete flexural members as per IRC 112:2020 have been evaluated and presented. Similar methodology can be adopted for evaluation of ductility and plastic rotations following the provisions of Eurocode-2.

### 2.2 Evaluation of design parameters for limiting conditions in flexure

#### *2.2.1 Maximum under-reinforced section i.e., sections with minimum amount of tension reinforcement*

The minimum percentage of tension reinforcement is different as per different standards. IS 456:2000[2] prescribes that minimum amount of tension reinforcement in beam should be $\frac{0.85}{f_y}bd$ whereas as per IS 13920:2016[7] this is $0.24\frac{\sqrt{f_{ck}}}{f_y}bd$, where the symbols have their standard meanings. IRC 112:2020[3] restricts the minimum amount of tension reinforcement in flexural members as –

$$A_{st,min} = 0.26\left(\frac{f_{ctm}}{f_{yk}}\right)b_t.d \quad \ldots (1)$$

$$= \rho_{min}.b_t.d \text{ but not less than } 0.0013\, b_t.d$$

where $\rho = p/100$ and $p$ is the percentage of tension reinforcement,

$b_t$ = mean width of the tension zone

$f_{ctm}$ = mean value of axial tensile strength of concrete

$f_{yk}$ =characteristic yield strength of reinforcement

The values of minimum percentage of tension reinforcement as per IRC have been calculated using equation 1 and the higher values between calculated $A_{st,min}$ and $0.0013\, b_t.d$ have been adopted. These calculated and adopted values for all permitted structural grades of concrete and steel have been presented in Table 1.

From this adopted $\rho_{min}$ corresponding depth of neutral axis$(x_{u,min})$ have been calculated using force equilibrium equation across a beam section as presented in Figures 1 and 2.

$$C = T$$
$$\text{or, } N.f_{ck}.x_{u,min}.b = 0.87f_y.A_{st,min}$$
$$\text{or, } N.f_{ck}.x_{u,min}.b = 0.87f_y.\rho_{min}bd$$

$$\text{or, } \left(\frac{x_{u,min}}{d}\right) = \frac{0.87f_y}{N.f_{ck}} \times \rho_{min} \quad \ldots (2)$$

Table 1 — Minimum percentage of tension reinforcement for flexural members as per IRC 112:2020.

| Grades of concrete ($f_{ck}$) | $\rho_{min}$ | | | | | | | |
|---|---|---|---|---|---|---|---|---|
| | Fe415/Fe415D/Fe415S | | Fe500/Fe500D/Fe500S | | Fe550/Fe550D | | Fe600 | |
| | Calculated | Adopted | Calculated | Adopted | Calculated | Adopted | Calculated | Adopted |
| M20 | 0.0012 | 0.0013 | 0.0010 | 0.0013 | 0.0009 | 0.0013 | 0.0008 | 0.0013 |
| M25 | 0.0014 | 0.0014 | 0.0011 | 0.0013 | 0.0010 | 0.0013 | 0.0010 | 0.0013 |
| M30 | 0.0016 | 0.0016 | 0.0013 | 0.0013 | 0.0012 | 0.0013 | 0.0011 | 0.0013 |
| M35 | 0.0018 | 0.0018 | 0.0015 | 0.0015 | 0.0013 | 0.0013 | 0.0012 | 0.0013 |
| M40 | 0.0019 | 0.0019 | 0.0016 | 0.0016 | 0.0014 | 0.0014 | 0.0013 | 0.0013 |
| M45 | 0.0021 | 0.0021 | 0.0017 | 0.0017 | 0.0016 | 0.0016 | 0.0014 | 0.0014 |
| M50 | 0.0022 | 0.0022 | 0.0018 | 0.0018 | 0.0017 | 0.0017 | 0.0015 | 0.0015 |
| M55 | 0.0023 | 0.0023 | 0.0019 | 0.0019 | 0.0017 | 0.0017 | 0.0016 | 0.0016 |
| M60 | 0.0025 | 0.0025 | 0.0021 | 0.0021 | 0.0019 | 0.0019 | 0.0017 | 0.0017 |
| M65 | 0.0028 | 0.0028 | 0.0023 | 0.0023 | 0.0021 | 0.0021 | 0.0019 | 0.0019 |
| M70 | 0.0028 | 0.0028 | 0.0023 | 0.0023 | 0.0021 | 0.0021 | 0.0020 | 0.0020 |
| M75 | 0.0029 | 0.0029 | 0.0024 | 0.0024 | 0.0022 | 0.0022 | 0.0020 | 0.0020 |
| M80 | 0.0030 | 0.0030 | 0.0025 | 0.0025 | 0.0023 | 0.0023 | 0.0021 | 0.0021 |
| M85 | 0.0031 | 0.0031 | 0.0025 | 0.0025 | 0.0023 | 0.0023 | 0.0021 | 0.0021 |
| M90 | 0.0031 | 0.0031 | 0.0026 | 0.0026 | 0.0024 | 0.0024 | 0.0022 | 0.0022 |

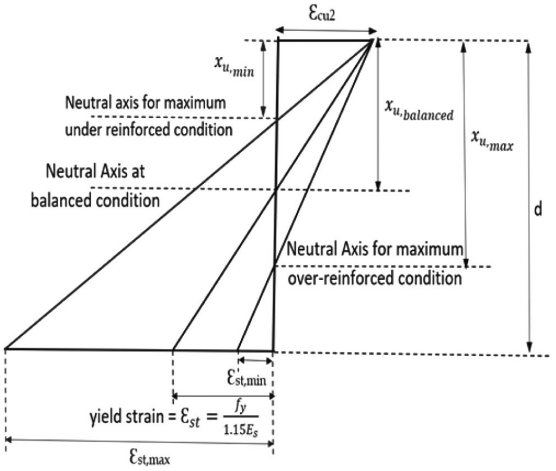


Fig. 1 — Strain distribution diagrams for maximum under-reinforced, balanced and maximum over-reinforced sections.

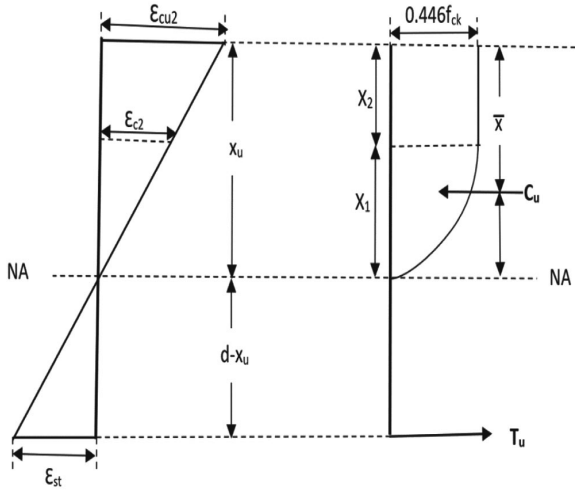


Fig. 2 — Strain distribution diagram and stress block for a beam section.

Table 2 — Compressive force on the section for various strength classes of concrete.

| Grades of Concrete ($f_{ck}$) | $C_u = N.f_{ck}.x_u.b$ |
|---|---|
| M 15 to 60 | $0.36\ f_{ck}.x_u.b$ |
| M65 | $0.351\ f_{ck}.x_u.b$ |
| M70 | $0.34\ f_{ck}.x_u.b$ |
| M75 | $0.328\ f_{ck}.x_u.b$ |
| M80 | $0.324\ f_{ck}.x_u.b$ |
| M85 | $0.314\ f_{ck}.x_u.b$ |
| M90 | $0.309\ f_{ck}.x_u.b$ |

N is the factor of compressive force which have been calculated for different strength classes of concrete and are presented in Table 2.

#### *2.2.2 Calculations of areas of stress blocks for all grades of concrete*

The limiting strain at the end of the parabolic portion of the stress block of concrete in compression is $\varepsilon_{c2}$ and that at the end of the rectangular portion of the stress block is $\varepsilon_{cu2}$. $x_2$ and $x_1$ denote the length of the rectangular and parabolic part of the stress block as shown in Figure 2.

From similar triangles, $\frac{x_1}{c2} = \frac{x_u}{cu2}$ and $x_2 = x_u - x_1$

The values of $x_1$ and $x_2$ for various strength classes of concrete have been calculated based on their stress-strain relationships. Let $C_u$ represent the compressive force. Thus, for a single lamina of the beam cross section, the compressive force is as expressed in equation 3.

$$C_u = (0.446f_{ck} \times x_2 \times b) + (\frac{2}{3} \times 0.446f_{ck} \times x_1 \times b) \quad \dots (3)$$

From eqn.-3, concrete compressive force ($C_u$) for all strength classes of concrete have been calculated and presented in Table 2.

Section will fail in flexure when the limiting strain ($\varepsilon_{cu2}$) in concrete in flexural compression is reached.[5,24] Since strain distribution diagram is linear as per Bernoulli's theorem, the line joining $\varepsilon_{cu2}$ with the calculated neutral axis depth will give the strain distribution diagram as shown in Figure 2, wherefrom the maximum strain in steel ($\varepsilon_{st,max}$) can be determined.

$$\varepsilon_{st,max} = \frac{\varepsilon_{cu2}}{\left(\frac{x_{u,min}}{d}\right)}\left[1 - \left(\frac{x_{u,min}}{d}\right)\right] \quad \dots (4)$$

From equations 2 and 4, the minimum depths of neutral axis and maximum strains in steel have been calculated and are presented in Table 3.

***2.2.3 Design parameters for balanced section***

In balanced condition the strain in steel reaches its yield strain and the strain in concrete reaches $\varepsilon_{cu2}$simultaneously. As per IRC 112:2020[3]the stress-strain relationships of steel are bilinear in nature having the yield stress of $0.87f_y$. The limiting or balanced values of strains can be calculated as $\frac{0.87f_y}{E_s}$, which are 0.0018, 0.0021, 0.0024, 0.0026 for Fe415/Fe415S/Fe415D, Fe500/Fe500S/Fe500D, Fe550/Fe550D and Fe 600 respectively. The line joining the concrete strain, $\varepsilon_{cu2}$ with the yield strain in steel gives the strain distribution diagram. From this strain distribution diagram of balanced section (similar to figure 2), it can be stated that-

$$\left(\frac{\varepsilon_{cu2}}{x_{u,bal}}\right) = \frac{\varepsilon_{st,balanced}}{d - x_{u,bal}}$$

$$x_{u,bal}(\varepsilon_{st,balanced} + \varepsilon_{cu2}) = \varepsilon_{cu2} \times d$$

$$\left(\frac{x_{u,bal}}{d}\right) = \frac{\varepsilon_{cu2}}{\varepsilon_{cu2}+\varepsilon_{st,balanced}} \quad \dots (5)$$

This $\left(\frac{x_{u,bal}}{d}\right)$is same for M20 to M60 grades of concrete as $\varepsilon_{cu2}$ is same for these concrete grades and will change for higher grades of concrete. This has been presented in Table 4. Now from stress block by equating the compressive force with tensile force, area of steel for balanced condition can be calculated as follows.

C = T

$$or, f_{st,balanced} \cdot A_{st,balanced} = N.f_{ck}.x_{u,bal}$$

$$or, 0.87f_y \times \frac{P_{t,balanced}bd}{100} = N.f_{ck}.x_{u,bal}.b$$

$$or, \rho_{balanced} = \frac{N.f_{ck}}{0.87f_y} \times \frac{x_{u,bal}}{d} \quad \dots (6)$$

Table 4 presents the calculated values of $\frac{x_{u,bal}}{d}$ and $\rho_{balanced}$for different grades of concrete

Table 3 — Minimum depths of neutral axis and maximum strains in steel in beam sections.

| Grades of concrete | Minimum depth of neutral axis and maximum strain in steel for $A_{st,min}$ | | | | | | | |
|---|---|---|---|---|---|---|---|---|
| | Fe415/Fe415D/Fe415S | | Fe500/Fe500D/Fe500S | | Fe550/Fe550D | | Fe600 | |
| | $\frac{x_{u,min}}{d}$ | $\varepsilon_{st,max}$ | $\frac{x_{u,min}}{d}$ | $\varepsilon_{st,max}$ | $\frac{x_{u,min}}{d}$ | $\varepsilon_{st,max}$ | $\frac{x_{u,min}}{d}$ | $\varepsilon_{st,max}$ |
| M20 | 0.06519 | 0.0502 | 0.078542 | 0.04106 | 0.086396 | 0.03701 | 0.09425 | 0.03364 |
| M25 | 0.05529 | 0.0598 | 0.062833 | 0.05220 | 0.069117 | 0.04714 | 0.0754 | 0.04292 |
| M30 | 0.05236 | 0.0633 | 0.052361 | 0.06334 | 0.057597 | 0.05727 | 0.062833 | 0.05220 |
| M35 | 0.05026 | 0.0661 | 0.050267 | 0.06613 | 0.050267 | 0.06613 | 0.053857 | 0.06149 |
| M40 | 0.04712 | 0.0708 | 0.047125 | 0.07077 | 0.047125 | 0.07077 | 0.047125 | 0.07077 |
| M45 | 0.04607 | 0.0725 | 0.046078 | 0.07246 | 0.046078 | 0.07246 | 0.046078 | 0.07246 |
| M50 | 0.04398 | 0.0761 | 0.043983 | 0.07608 | 0.043983 | 0.07608 | 0.043983 | 0.07608 |
| M55 | 0.04227 | 0.0793 | 0.04227 | 0.07930 | 0.04227 | 0.07930 | 0.04227 | 0.07930 |
| M60 | 0.04188 | 0.0801 | 0.041889 | 0.08005 | 0.041889 | 0.08005 | 0.041889 | 0.08005 |
| M65 | 0.04357 | 0.0728 | 0.043575 | 0.07278 | 0.043575 | 0.07278 | 0.043575 | 0.07278 |
| M70 | 0.04270 | 0.0696 | 0.042707 | 0.06960 | 0.042707 | 0.06960 | 0.042707 | 0.06960 |
| M75 | 0.04320 | 0.0642 | 0.043205 | 0.06420 | 0.043205 | 0.06420 | 0.043205 | 0.06420 |
| M80 | 0.04190 | 0.0638 | 0.041904 | 0.06384 | 0.041904 | 0.06384 | 0.041904 | 0.06384 |
| M85 | 0.04154 | 0.0621 | 0.041548 | 0.06211 | 0.041548 | 0.06211 | 0.041548 | 0.06211 |
| M90 | 0.04069 | 0.0617 | 0.040699 | 0.06174 | 0.040699 | 0.06174 | 0.040699 | 0.06174 |

Table 4 — Balanced depth of neutral axis and balanced percentages of steel as per IRC 112:2020

| Grades of Concrete | $\varepsilon_{cu2}$ | Grades of Steel | | | | | | | |
|---|---|---|---|---|---|---|---|---|---|
| | | Fe415/Fe415D/Fe415S | | Fe500/Fe500D/Fe500S | | Fe550/Fe550D | | Fe600 | |
| | | $\frac{x_{u,bal}}{d}$ | $\rho_{balanced}$ | $\frac{x_{u,bal}}{d}$ | $\rho_{balanced}$ | $\frac{x_{u,bal}}{d}$ | $\rho_{balanced}$ | $\frac{x_{u,bal}}{d}$ | $\rho_{balanced}$ |
| M20 | 0.0035 | 0.6597 | 0.0132 | 0.6167 | 0.0102 | 0.5940 | 0.0089 | 0.5728 | 0.0079 |
| M25 | 0.0035 | 0.6597 | 0.0164 | 0.6167 | 0.0128 | 0.5940 | 0.0112 | 0.5728 | 0.0099 |
| M30 | 0.0035 | 0.6597 | 0.0197 | 0.6167 | 0.0153 | 0.5940 | 0.0134 | 0.5728 | 0.0119 |
| M35 | 0.0035 | 0.6597 | 0.0230 | 0.6167 | 0.0179 | 0.5940 | 0.0156 | 0.5728 | 0.0138 |
| M40 | 0.0035 | 0.6597 | 0.0263 | 0.6167 | 0.0204 | 0.5940 | 0.0179 | 0.5728 | 0.0158 |
| M45 | 0.0035 | 0.6597 | 0.0296 | 0.6167 | 0.0230 | 0.5940 | 0.0201 | 0.5728 | 0.0178 |
| M50 | 0.0035 | 0.6597 | 0.0329 | 0.6167 | 0.0255 | 0.5940 | 0.0223 | 0.5728 | 0.0198 |
| M55 | 0.0035 | 0.6597 | 0.0362 | 0.6167 | 0.0281 | 0.5940 | 0.0246 | 0.5728 | 0.0217 |
| M60 | 0.0035 | 0.6597 | 0.0395 | 0.6167 | 0.0306 | 0.5940 | 0.0268 | 0.5728 | 0.0237 |
| M65 | 0.0033 | 0.6464 | 0.0409 | 0.6027 | 0.0316 | 0.5797 | 0.0277 | 0.5584 | 0.0244 |
| M70 | 0.0031 | 0.6320 | 0.0417 | 0.5877 | 0.0322 | 0.5644 | 0.0281 | 0.5429 | 0.0248 |
| M75 | 0.0029 | 0.6163 | 0.0420 | 0.5714 | 0.0323 | 0.5479 | 0.0282 | 0.5263 | 0.0248 |
| M80 | 0.0028 | 0.6080 | 0.0436 | 0.5628 | 0.0335 | 0.5392 | 0.0292 | 0.5176 | 0.0257 |
| M85 | 0.0027 | 0.5993 | 0.0443 | 0.5538 | 0.0340 | 0.5302 | 0.0296 | 0.5085 | 0.0260 |
| M90 | 0.0026 | 0.5902 | 0.0454 | 0.5445 | 0.0348 | 0.5208 | 0.0302 | 0.4990 | 0.0266 |

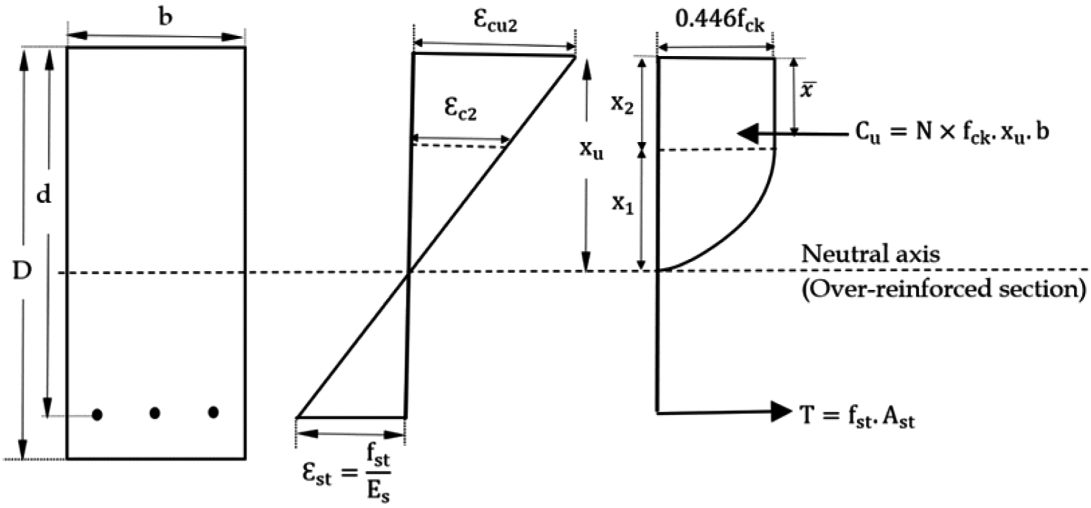


Fig. 3 — Strain distribution diagram and stress block for over-reinforced section.

and steel, which have been obtained from equations 5 and 6, respectively.

***2.2.4 Design parameters for over-reinforced sections***

For over-reinforced sections, since steel is not reaching the yield point, the stress in steel will not be constant and will vary linearly with strain following the first line (linear elastic region) of the bilinear stress-strain relationship of steel. Strain in steel will depend upon the level of over-reinforcement. Hence for over-reinforced sections only one point in the strain distribution diagram is known i.e., strain at the outermost fibre in concrete is reached $\varepsilon_{cu2}$. Neither the depth of neutral axis nor the strain in steel is known. Using the force equilibrium equation, from stress and strain distribution diagram as presented in Figure 3, two unknowns can be evaluated. The process of solution is described below.

From Figure-3 it can be stated that, as per force equilibrium condition,

$$C = T$$
$$\therefore N \times f_{ck}.x_u.b = f_{st}.A_{st}$$

where, N is the factor of area of the stress block of concrete, which presented in Table-2. Substituting

$A_{st} = \frac{pbd}{100}$ equation will be as follows.

$$N \times f_{ck}.x_u.b = f_{st}.\frac{pbd}{100}$$

$$or, \quad f_{st} = \frac{N\, f_{ck}.x_u.b \times 100}{pbd}$$

$$or, f_{st} = \frac{\left\{100\, N\, f_{ck} \times \left(\frac{x_u}{d}\right)\right\}}{p} \quad \ldots (7)$$

From strain distribution diagram,

$$\frac{\varepsilon_{cu2}}{x_u} = \frac{\varepsilon_{st}}{d - x_u}$$

or, $\frac{\varepsilon_{cu2}}{x_u} = \frac{f_{st}}{E_s(d-x_u)}$ where, $\frac{f_{st}}{E_s} = \varepsilon_{st}$

$$\text{or, } f_{st} = \left\{\frac{E_s \times \varepsilon_{cu2}}{\frac{x_u}{d}}\right\}.\left(1 - \frac{x_u}{d}\right) \quad \ldots (8)$$

Now by equating equations 7 and 8,

$$\frac{\left\{100.N.f_{ck} \times \left(\frac{x_u}{d}\right)\right\}}{p} = \left\{\frac{E_s \times \varepsilon_{cu2}}{\frac{x_u}{d}}\right\}.\left(1 - \frac{x_u}{d}\right)$$

Let $\left(\frac{x_u}{d}\right)$=k

$$\text{Hence, } \frac{\{100.N.f_{ck} \times k\}}{p} = \left\{\frac{E_s \times \varepsilon_{cu2}}{k}\right\}.(1-k)$$

$$\text{or, } 1 - k = \left[\frac{100.N.f_{ck}}{p \times \varepsilon_{cu2} \times E_s}\right].k^2$$

$$\text{or, } \left[\frac{100.N.f_{ck}}{p \times \varepsilon_{cu2} \times E_s}\right] k^2 + k - 1 = 0 \quad \ldots (9)$$

By solving this quadratic equation, values of k i.e., $\frac{x_u}{d}$ for different grades of concrete for over-reinforced sections can be determined.

### 2.3 Maximum permitted section condition of the flexural members

As per IS 456:2000[2] over-reinforced sections are not permitted in flexure. However, IRC 112:2020[3] does not restrict the type of sections, hence under-reinforced, balanced and over-reinforced sections all are permitted in flexural design. But the maximum reinforcement percentage allowed in the section is restricted by the code.

#### *2.3.1 Maximum percentage of tension reinforcement as per IRC 112:2020*

The maximum area of tension reinforcement for beams is 2.5% of the area of concrete. i.e.,

$A_{st} = 2.5\%$ of $A_c$

The maximum reinforcement is converted in terms of the effective cross-section, i.e., width 'b' and effective depth 'd' as per the following expression -

$$A_{st,max} = \left(\frac{2.5}{100}\right) \times A_c$$

$$or, A_{st} = \left(\frac{2.5}{100}\right) \times (A_{gross} - A_{st})$$

Hence, $A_{st} = 0.025A_{gross} - 0.025A_{st}$

$$A_{st}\,(1 + 0.025) = 0.025bD$$

or, $A_{st} = \frac{0.025}{(1+0.025)}$bD

or, $A_{st} = 0.02439$ bD

$A_{effective} = b \times d$, and assuming effective depth, d=0.9D.[1,25]

$$A_{st} = \left(\frac{0.02439}{0.9}\right) bd$$

$$\therefore A_{st} = 0.0271 \times bd$$

Hence the area of steel expressed in terms of percentage of effective cross-sectional area (bd) is 2.71.

#### *2.3.2 Maximum permitted section in flexure as per IRC 112:2020*

The maximum percentage of tension reinforcement ($p_{t,max}$) as per IRC 112:2020[3] is 2.71. It can be stated that for any beam section if the value of $p_{t,max}$ is greater than the $p_{t,balanced}$, in that case, the maximum possible condition of the section will be over-reinforced. Thus, the standard permits the design of over-reinforced condition. Whereas if $p_{t,max}$ is less than $p_{t,balanced}$, the maximum possible condition of the section is restricted to under-reinforced condition. In this case the design of over-reinforced section is not permitted by the standard. This has been clearly shown in Figure 4.

For different grades of concrete these maximum possible conditions are different and these have been presented in Table 5.

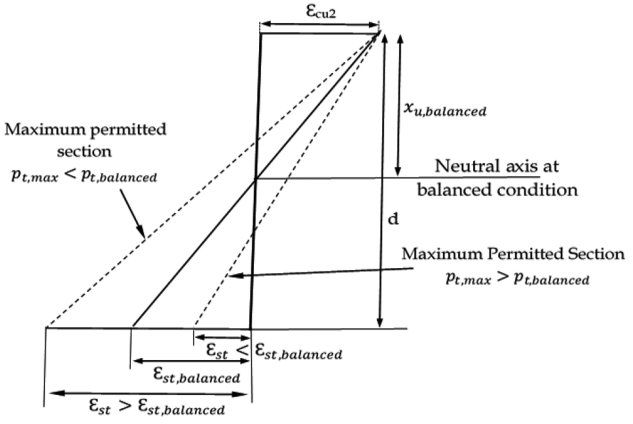


Fig. 4 — Strain distribution diagram for different maximum permitted sections in flexure as per IRC 112:2020.

Table 5 — Maximum possible condition for different reinforced concrete sections.

| Grades of concrete | Fe415/Fe415D/Fe415S | | | | Fe500/Fe500D/Fe500S | | | |
|---|---|---|---|---|---|---|---|---|
| | $p_{t_{balanced}}$ | $p_{t_{max}}$ | $\frac{x_{u_{max}}}{d}$ | Maximum permitted section condition | $p_{t_{balanced}}$ | $p_{t_{max}}$ | $\frac{x_{u_{max}}}{d}$ | Maximum permitted section condition |
| M20 | 1.316 | 2.71 | 0.773 | Over-reinforced allowed | 1.021 | 2.71 | 0.773 | Over-reinforced allowed |
| M25 | 1.645 | | 0.740 | | 1.276 | | 0.740 | |
| M30 | 1.973 | | 0.712 | | 1.531 | | 0.712 | |
| M35 | 2.302 | | 0.687 | | 1.786 | | 0.687 | |
| M40 | 2.631 | | 0.665 | | 2.042 | | 0.665 | |
| M45 | 2.960 | | 0.604 | Under-reinforced allowed | 2.297 | | 0.645 | |
| M50 | 3.289 | | 0.544 | | 2.552 | | 0.627 | |
| M55 | 3.618 | | 0.494 | | 2.807 | | 0.494 | Under-reinforced allowed |
| M60 | 3.947 | | 0.453 | | 3.062 | | 0.453 | |
| M65 | 4.089 | | 0.428 | | 3.165 | | 0.428 | |
| M70 | 4.172 | | 0.411 | | 3.220 | | 0.411 | |
| M75 | 4.201 | | 0.398 | | 3.232 | | 0.398 | |
| M80 | 4.363 | | 0.378 | | 3.352 | | 0.378 | |
| M85 | 4.428 | | 0.367 | | 3.397 | | 0.367 | |
| M90 | 4.543 | | 0.352 | | 3.478 | | 0.352 | |
| Grades of concrete | Fe550/Fe550D | | | | Fe 600 | | | |
| | $p_{t_{balanced}}$ | $p_{t_{max}}$ | $\frac{x_{u_{max}}}{d}$ | Maximum permitted section condition | $p_{t_{balanced}}$ | $p_{t_{max}}$ | $\frac{x_{u_{max}}}{d}$ | Maximum permitted section condition |
| M20 | 0.894 | 2.71 | 0.773 | Over-reinforced allowed | 0.790 | 2.71 | 0.773 | Over-reinforced allowed |
| M25 | 1.117 | | 0.740 | | 0.988 | | 0.740 | |
| M30 | 1.341 | | 0.712 | | 1.185 | | 0.712 | |
| M35 | 1.564 | | 0.687 | | 1.383 | | 0.687 | |
| M40 | 1.788 | | 0.665 | | 1.580 | | 0.665 | |
| M45 | 2.011 | | 0.645 | | 1.778 | | 0.645 | |
| M50 | 2.234 | | 0.627 | | 1.975 | | 0.627 | |
| M55 | 2.458 | | 0.611 | | 2.173 | | 0.611 | |
| M60 | 2.681 | | 0.596 | | 2.370 | | 0.596 | |
| M65 | 2.835 | | 0.568 | Under-reinforced allowed | 2.443 | | 0.575 | |
| M70 | 2.972 | | 0.544 | | 2.479 | | 0.558 | |
| M75 | 3.092 | | 0.527 | | 2.722 | | 0.575 | Under-reinforced allowed |
| M80 | 3.246 | | 0.500 | | 2.856 | | 0.546 | |
| M85 | 3.391 | | 0.486 | | 2.98 | | 0.530 | |
| M90 | 3.526 | | 0.467 | | 3.098 | | 0.509 | |

## 3 Results and Discussion

Evaluation of ductility for different types of sections The principle for evaluation of ductility is based on load-deformation response. Depending on the types of deformations, ductility can be of different types i.e., Strain ductility, Displacement ductility, Curvature ductility, Rotational ductility. It can be measured by the ratio of deformation at

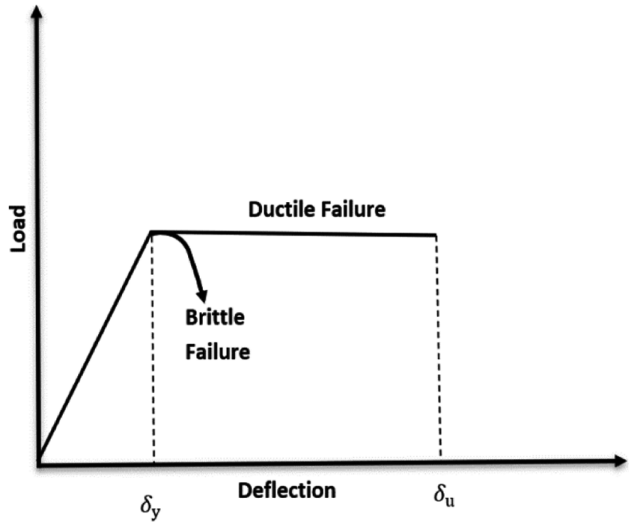


Fig. 5 — Load deflection behavior of flexural members.

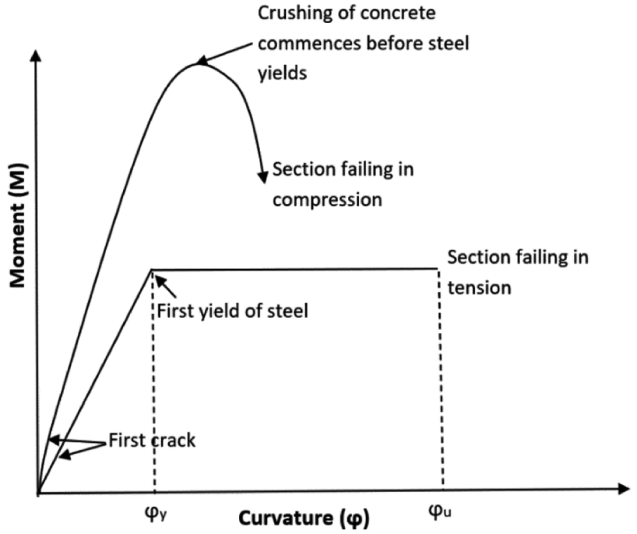


Fig. 6 — Idealized moment curvature relationship of a section in flexure failing in tension and compression[26].

ultimate to the deformation at yield stage (refer Figure 5 and 6).

### 3.1 Evaluation of strain ductility for maximum under-reinforced sections

The strain ductility of a section can be expressed as the ratio of the maximum or ultimate strain to the yield strain, which is the minimum strain at which the steel starts to yield.

$$\mu_\varepsilon = \frac{\text{st,max}}{\text{st,y}}$$

where, the ultimate strain, in the tension steel, $_{\text{st,max}}$, is achieved when the depth of the neutral axis is at its minimum value, i.e., $(x_{u,min})$. This minimum depth of neutral axis corresponds to the minimum percentage of tension reinforcement, $A_{st,min}$. This has been clearly presented in figure-1. Minimum percentage of tension reinforcement as per IRC 112:2020[3] has already been calculated in Table 1. $_{st,y}$is the steel strain at the yield stage, and this will be achieved when section is having balanced percentage of tension reinforcement. Hence,

$$_{\text{st,y}} = \ _{\text{st,balanced}} = \frac{f_y}{1.15E_s}$$

Strain ductility values for all concrete and steel grades as per IRC 112:2020[3] have been presented in Table 6.

When designing RC sections, the horizontal plastic branch of the stress-strain curve of steel has no limit on strain values. This means that a significant amount of yielding or deformation may occur for the development of the concrete stress block, resulting in an increase in curvature of the section which may not be practical or feasible for RC sections with larger depths[1]. However, since the actual percentage of steel used in construction is typically higher than the minimum required steel percentage, the actual rotation values will be lower than the values calculated using $A_{st,min}$. It is observed that the strain ductility values for maximum under-reinforced section as per IRC 112[3] is ranging between 12.89 to 44.35. The research work by Jha and Bhanja stated that, maximum under-reinforced sections as per IS 456:2000[2] has strain ductility range from 6.62 to 25.98[1], whereas as per IS 13920:2016[6], the corresponding parameter varied from 4.51 to 10.12.[27] The strain ductility is inversely proportional to the strength of steel. On the other hand, for concrete grades up to M60, strain ductility increases with increase in concrete strength. However, beyond M60, the strain ductility tends to decrease as the strength of concrete increases.

### 3.2 Evaluation of curvature ductility and plastic rotations

Reinforced concrete sections subjected to flexure only, fail when the compressive strain in concrete reaches its limiting strain and the entire stress block in the compression zone develops, leading to crushing of the concrete. In the limit state design approach, sections are designed to go beyond their yield stage and failure occurs in the post-yield region. The initiation of failure is referred to as Stage-I or the yield stage, while ultimate failure is referred to as

Table 6 — Strain ductility ($\mu_\varepsilon$) values of sections with minimum area of tension reinforcement as per IRC 112:2020.

| Grades of concrete ($f_{ck}$) | Strain ductility ($\mu_\varepsilon$) | | | |
|---|---|---|---|---|
| | Fe415/Fe415D/Fe415S | Fe500/Fe500D/Fe500S | Fe 550/Fe550D | Fe 600 |
| M20 | 27.80 | 18.88 | 15.47 | 12.89 |
| M25 | 33.12 | 24.00 | 19.70 | 16.44 |
| M30 | 35.09 | 29.12 | 23.94 | 20.00 |
| M35 | 36.63 | 30.40 | 27.64 | 23.56 |
| M40 | 39.20 | 32.54 | 29.58 | 27.12 |
| M45 | 40.14 | 33.31 | 30.29 | 27.76 |
| M50 | 42.14 | 34.98 | 31.80 | 29.15 |
| M55 | 43.93 | 36.46 | 33.15 | 30.38 |
| M60 | 44.35 | 36.81 | 33.46 | 30.67 |
| M65 | 40.12 | 33.30 | 30.27 | 27.75 |
| M70 | 38.49 | 31.95 | 29.04 | 26.62 |
| M75 | 35.58 | 29.53 | 26.84 | 24.61 |
| M80 | 35.46 | 29.43 | 26.76 | 24.53 |
| M85 | 34.50 | 28.64 | 26.03 | 23.86 |
| M90 | 33.95 | 28.18 | 25.61 | 23.48 |

Stage-II or the ultimate stage [1,26].

Curvature ductility ($\mu_\varphi$) of the section can be calculated as,

$$\mu_\phi = \frac{\text{Curvature at ultimate stage}}{\text{Curvature at yield stage}} = \frac{\phi_u}{\phi_y}$$

The plastic curvature ($\phi_p$) of any reinforced concrete section can be calculated as,

$$\phi_p = (\text{Curvature at ultimate} - \text{Curvature at yield})$$

or, $\phi_p = (\phi_u - \phi_y)$

Curvature may be defined as rotation per unit length. $\text{Curvature } (\phi) = \frac{\text{Rotation } (\theta)}{\text{Length } (l)}$

Hence,

$$\text{plastic curvature } (\phi_p) = \frac{\text{plastic rotation capacity } (\theta_p)}{\text{Length of plastic hinge } (l_p)}$$

$$\therefore \theta_p = \phi_p \times l_p$$

Hence, Plastic rotation, $\theta_p = (\phi_u - \phi_y) \times l_p$

Plastic hinge($l_p$) in reinforced concrete members refers to a specific section of the member where the concrete undergoes plastification in compression, resulting in the rotation of the section under a constant ultimate moment, while the steel in the tension zone continues to yield.[22,28] In a particular section, the moment at which a plastic hinge forms, is known as the section plastic moment ($M_p$).[29] The term "plastic hinge" is used because the hinge forms due to the plastification of the materials. Various researchers have put forth different lengths for plastic hinges. The recommended length is $l_p = \frac{d}{2}$, which is widely regarded as an acceptable value leading to conservative outcomes. In this context, 'd' represents the section depth in the direction of loading.[30,31,32,33] The formation of plastic hinges reduces the stiffness of the structure, leading to significant increase in deflections. This approach ensures improved accuracy in predicting deflection, curvature, and plastic rotation capacity in such members. Additionally, the formation of plastic hinges significantly influences the behaviour and failure mechanism of flexural members[10,34]

This has been considered to calculate plastic rotation of the sections.

$$\therefore \theta_p = (\phi_u - \phi_y) \times \frac{d}{2} \quad \ldots (10)$$

By following these concepts curvature ductility and plastic rotations for three critical types of sections have been evaluated, which have been briefly discussed in the subsequent sections.

#### *3.2.1 Evaluation of ductility and plastic rotations for maximum under-reinforced sections*

Figure 7 illustrates the strain distribution diagram and stress distribution of an under-reinforced section. At the failure stage, the concrete reaches its ultimate strain of $\varepsilon_{cu2}$, and steel reaches its maximum strain of $\varepsilon_{st,max}$. The end of the elastic phase, which is known as the yield stage, is depicted in Stage-I, and the curvature at this point is referred to as the yield curvature. On the other hand, Stage-II represents the

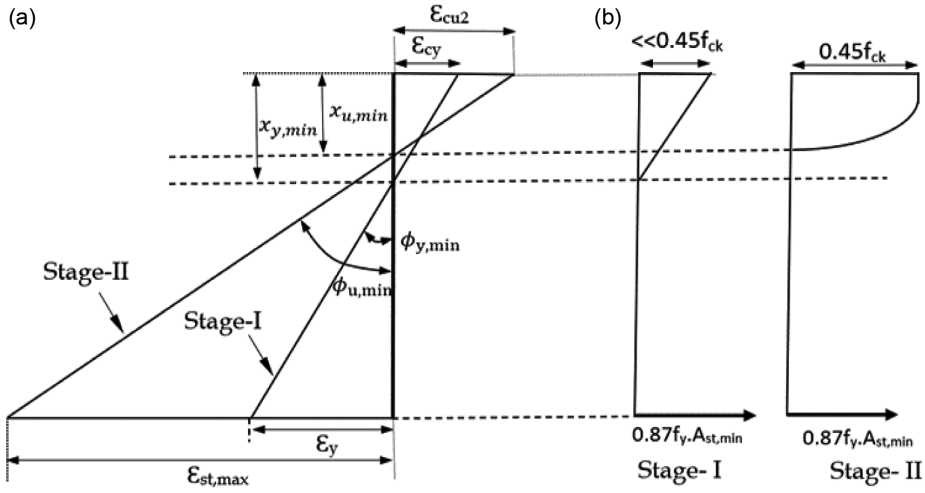


Fig. 7 — (a) Strain distribution diagram and (b) Stress blocks for failure in maximum under-reinforced condition.

Table 7 — Neutral axis depths at yield stage and corresponding yield curvatures for maximum under-reinforced sections according to IRC 112:2020.

| Grades of concrete | Fe415/Fe415D/Fe415S | | Fe500/Fe500D/Fe500S | | Fe550/Fe550D | | Fe600 | |
|---|---|---|---|---|---|---|---|---|
| | $\left(\frac{x_{y,min}}{d}\right)$ | $\phi_{y,min} \times d$ | $\left(\frac{x_{y,min}}{d}\right)$ | $\phi_{y,min} \times d$ | $\left(\frac{x_{y,min}}{d}\right)$ | $\phi_{y,min} \times d$ | $\left(\frac{x_{y,min}}{d}\right)$ | $\phi_{y,min} \times d$ |
| M20 | 0.1252 | 0.00206 | 0.1252 | 0.00249 | 0.1252 | 0.00274 | 0.1252 | 0.002984 |
| M25 | 0.1267 | 0.00207 | 0.1233 | 0.00248 | 0.1233 | 0.00273 | 0.1233 | 0.002977 |
| M30 | 0.1324 | 0.00208 | 0.1214 | 0.00248 | 0.1214 | 0.00272 | 0.1214 | 0.002971 |
| M35 | 0.1375 | 0.00209 | 0.1261 | 0.00249 | 0.1206 | 0.00272 | 0.1196 | 0.002965 |
| M40 | 0.1400 | 0.00210 | 0.1284 | 0.00250 | 0.1228 | 0.00273 | 0.1179 | 0.002959 |
| M45 | 0.1443 | 0.00211 | 0.1323 | 0.00251 | 0.1266 | 0.00274 | 0.1216 | 0.002971 |
| M50 | 0.1463 | 0.00211 | 0.1342 | 0.00251 | 0.1284 | 0.00274 | 0.1233 | 0.002977 |
| M55 | 0.1481 | 0.00212 | 0.1359 | 0.00252 | 0.1300 | 0.00275 | 0.1249 | 0.002982 |
| M60 | 0.1516 | 0.00213 | 0.1391 | 0.00253 | 0.1331 | 0.00276 | 0.1278 | 0.002993 |
| M65 | 0.1565 | 0.00214 | 0.1436 | 0.00254 | 0.1374 | 0.00277 | 0.1320 | 0.003007 |
| M70 | 0.1581 | 0.00214 | 0.1451 | 0.00254 | 0.1389 | 0.00278 | 0.1334 | 0.003012 |
| M75 | 0.1593 | 0.00215 | 0.1463 | 0.00255 | 0.1400 | 0.00278 | 0.1345 | 0.003015 |
| M80 | 0.1590 | 0.00215 | 0.1460 | 0.00255 | 0.1397 | 0.00278 | 0.1342 | 0.003015 |
| M85 | 0.1605 | 0.00215 | 0.1474 | 0.00255 | 0.1411 | 0.00279 | 0.1355 | 0.003019 |
| M90 | 0.1602 | 0.00215 | 0.1471 | 0.00255 | 0.1408 | 0.00278 | 0.1352 | 0.003018 |

ultimate or failure stage, and the curvature at this point is known as the ultimate curvature[1].

3.2.1.1 Stage-I or yield stage

At Stage-I, the concrete strain ($\varepsilon_{cy}$) is lower than the limiting strain $\varepsilon_{c2}$ and the corresponding stress will be lower than 0.446 $f_{ck}$. The steel strain at this stage is the yield strain, which is $\varepsilon_{st,y} = \frac{0.87f_y}{E_s}$. Since the strain levels in concrete at this stage are very small, calculations have been performed following the linear elastic theory.[35,36,37] Depth of the neutral axis at this stage termed as $x_{y,min}$, can be calculated by considering moments for areas of compression and tension about the neutral axis of the transformed or equivalent concrete section. Park and Paulay established an equation based on the elastic method, which can be used to calculate the depth of the neutral axis at this stage.[26]

$$\left(\frac{x_{y,min}}{d}\right) = -(m\rho) + \sqrt{(m\rho)^2 + 2(m\rho)} \quad \ldots (11)$$

where, $m = \text{modular ratio} = \frac{E_s}{E_{cm}}$

IRC 112:2020[3] provides values of $E_{cm}$, which is the modulus of elasticity of concrete.

$E_s$= Design value of modulus of elasticity of reinforcing steel

ρ is the tension reinforcement ratio

Table 7 presents the values of $\frac{x_{y,min}}{d}$ for various grades of concrete and steel, which have been calculated using equation 11. Using the concept of

Table 8 — Neutral axis depths and curvatures at failure or ultimate stage for different grades of concrete and steel for maximum under-reinforced sections as per IRC 112.

| Grades of Concrete | Ultimate curvature for different grades of concrete and steel | | | | | | | |
|---|---|---|---|---|---|---|---|---|
| | Fe415/Fe415D/Fe415S | | Fe500/Fe500D/Fe500S | | Fe550/Fe550D | | Fe600 | |
| | $\frac{x_{u,min}}{d}$ | $\phi_{u,min} \times d$ | $\frac{x_{u,min}}{d}$ | $\phi_{u,min} \times d$ | $\frac{x_{u,min}}{d}$ | $\phi_{u,min} \times d$ | $\frac{x_{u,min}}{d}$ | $\phi_{u,min} \times d$ |
| M20 | 0.065 | 0.0537 | 0.079 | 0.0446 | 0.086 | 0.0405 | 0.094 | 0.0371 |
| M25 | 0.055 | 0.0633 | 0.063 | 0.0557 | 0.069 | 0.0506 | 0.075 | 0.0464 |
| M30 | 0.052 | 0.0668 | 0.052 | 0.0668 | 0.058 | 0.0608 | 0.063 | 0.0557 |
| M35 | 0.050 | 0.0696 | 0.050 | 0.0696 | 0.050 | 0.0696 | 0.054 | 0.0650 |
| M40 | 0.047 | 0.0743 | 0.047 | 0.0743 | 0.047 | 0.0743 | 0.047 | 0.0743 |
| M45 | 0.046 | 0.0760 | 0.046 | 0.0760 | 0.046 | 0.0760 | 0.046 | 0.0760 |
| M50 | 0.044 | 0.0796 | 0.044 | 0.0796 | 0.044 | 0.0796 | 0.044 | 0.0796 |
| M55 | 0.042 | 0.0828 | 0.042 | 0.0828 | 0.042 | 0.0828 | 0.042 | 0.0828 |
| M60 | 0.042 | 0.0836 | 0.042 | 0.0836 | 0.042 | 0.0836 | 0.042 | 0.0836 |
| M65 | 0.044 | 0.0757 | 0.044 | 0.0757 | 0.044 | 0.0757 | 0.044 | 0.0757 |
| M70 | 0.043 | 0.0726 | 0.043 | 0.0726 | 0.043 | 0.0726 | 0.043 | 0.0726 |
| M75 | 0.043 | 0.0671 | 0.043 | 0.0671 | 0.043 | 0.0671 | 0.043 | 0.0671 |
| M80 | 0.042 | 0.0668 | 0.042 | 0.0668 | 0.042 | 0.0668 | 0.042 | 0.0668 |
| M85 | 0.042 | 0.0650 | 0.042 | 0.0650 | 0.042 | 0.0650 | 0.042 | 0.0650 |
| M90 | 0.041 | 0.0639 | 0.041 | 0.0639 | 0.041 | 0.0639 | 0.041 | 0.0639 |

similar triangles, curvature ($\phi_{y,min}$) of sections at yield stage has been calculated, by using equation 12.

$$\phi_{y,min} = \frac{\varepsilon_{st,y}}{d - x_{y,min}} \quad \ldots (12)$$

The values are shown in Table 7 (Refer Figure 7).

**Sample Calculation:**

In case of M40 grade of concrete, and Fe 500 steel, $\rho_{min}$=0.00156 (Refer Table 1),

$$m = \frac{E_s}{E_{cm}} = \frac{2 \times 10^5}{33 \times 10^3} = 6.06$$

By substituting these values in equation 11,

$$\left(\frac{x_{y,min}}{d}\right) = -(6.06 \times 0.00156) + \left[(6.06 \times 0.00156)^2 + 2(6.06 \times 0.00156)\right]^{1/2}$$

$$\left(\frac{x_{y,min}}{d}\right) = 0.12838$$

Hence, $\phi_{y,min} = \frac{\varepsilon_{st,y}}{d - x_{y,min}} = \frac{\varepsilon_{st,y}}{d\left(1 - \frac{x_{y,min}}{d}\right)}$

$$\therefore \phi_{y,min} = \frac{0.002175}{d(1 - 0.12838)} = \frac{0.0024954}{d}$$

3.2.1.2 Stage-II- At failure stage

The ultimate stage, also known as the collapse stage, is characterized by the ultimate curvature. At this stage, the strain in steel ($\varepsilon_{st,max}$) exceeds the yield strain and continues to increase until the compressive strain ($\varepsilon_c$) at the outermost concrete reaches $_{cu2}$, resulting in the development of the entire compressive stress block in concrete.[1,27,35] On the other hand, the stress in tension steel remains constant after yielding. The force equilibrium equation can be used to determine the values of $\frac{x_{u,min}}{d}$ for various strength classes of concrete and steel. These values have already been computed and presented in Table 2. Curvature at this stage can be calculated as follows.

$$\phi_{u,min} = \left(\frac{\varepsilon_{cu2}}{x_{u,min}}\right) = \left(\frac{\varepsilon_{cu2}}{\frac{x_{u,min}}{d} \times d}\right) \quad \ldots (13)$$

Using the values of $\left(\frac{x_{u,min}}{d}\right)$ and $\varepsilon_{cu2}$, the ultimate curvatures at this stage have been calculated and shown in Table 8 (Refer Figure 7).

**Sample Calculation:**

In case of M40 grade of concrete, and Fe 500 steel,

$\varepsilon_{cu2} = 0.0035$, $\frac{x_{u,min}}{d} = 0.047125$ (Table 2)

$$\therefore \phi_{u,min} = \left(\frac{0.0035}{0.047125d}\right) = \frac{0.07427}{d}$$

Curvature ductility ($\mu_\varphi$) of maximum under-reinforced section can be calculated as,

Table 9 — Curvature ductility and plastic rotations for maximum under-reinforced sections.

| Grades of concrete | Curvature ductility and plastic rotations | | | | | | | |
|---|---|---|---|---|---|---|---|---|
| | Fe415/Fe415D/Fe415S | | Fe500/Fe500D/Fe500S | | Fe550/Fe550D | | Fe600 | |
| | Curvature Ductility ($\mu_\varphi$) | Plastic Rotation ($\theta_p$) (Radian) | Curvature Ductility ($\mu_\varphi$) | Plastic Rotation ($\theta_p$) (Radian) | Curvature Ductility ($\mu_\varphi$) | Plastic Rotation ($\theta_p$) (Radian) | Curvature Ductility ($\mu_\varphi$) | Plastic Rotation ($\theta_p$) (Radian) |
| 20 | 26.02 | 0.02581 | 17.92 | 0.02104 | 14.81 | 0.01889 | 12.45 | 0.01708 |
| 25 | 30.62 | 0.03062 | 22.45 | 0.02661 | 18.56 | 0.02396 | 15.59 | 0.02172 |
| 30 | 32.12 | 0.03238 | 27.00 | 0.03218 | 22.32 | 0.02902 | 18.75 | 0.02637 |
| 35 | 33.27 | 0.03377 | 27.98 | 0.03357 | 25.59 | 0.03345 | 21.92 | 0.03101 |
| 40 | 35.38 | 0.03609 | 29.76 | 0.03589 | 27.23 | 0.03577 | 25.10 | 0.03566 |
| 45 | 36.01 | 0.03692 | 30.30 | 0.03673 | 27.73 | 0.03661 | 25.56 | 0.03649 |
| 50 | 37.63 | 0.03873 | 31.68 | 0.03853 | 28.99 | 0.03842 | 26.73 | 0.03830 |
| 55 | 39.07 | 0.04034 | 32.90 | 0.04014 | 30.11 | 0.04003 | 27.76 | 0.03991 |
| 60 | 39.27 | 0.04071 | 33.07 | 0.04051 | 30.27 | 0.04040 | 27.92 | 0.04028 |
| 65 | 35.39 | 0.03680 | 29.82 | 0.03660 | 27.30 | 0.03648 | 25.19 | 0.03636 |
| 70 | 33.85 | 0.03522 | 28.53 | 0.03502 | 26.13 | 0.03490 | 24.10 | 0.03479 |
| 75 | 31.26 | 0.03249 | 26.35 | 0.03229 | 24.13 | 0.03217 | 22.26 | 0.03205 |
| 80 | 31.13 | 0.03234 | 26.24 | 0.03214 | 24.03 | 0.03202 | 22.17 | 0.03190 |
| 85 | 30.22 | 0.03142 | 25.47 | 0.03122 | 23.33 | 0.03110 | 21.53 | 0.03098 |
| 90 | 29.72 | 0.03087 | 25.05 | 0.03067 | 22.94 | 0.03055 | 21.17 | 0.03043 |

$$\mu_\phi = \frac{\phi_{u,min}}{\phi_{y,min}} = \frac{\phi_{u,min} \times d}{\phi_{y,min} \times d} \quad \ldots (14)$$

The plastic rotation ($\theta_p$) of any under-reinforced concrete beam section can be calculated as,

$$\therefore \theta_p = \left(\phi_{u,min} - \phi_{y,min}\right) \times \frac{d}{2}$$

$$\theta_p = \left(\phi_{u,min} \times d\right) - \left(\phi_{y,min} \times d\right) \times \frac{1}{2} \quad \ldots (15)$$

By using equation 14 and 15 the curvature ductility and plastic rotations values have been evaluated, which are presented in Table 9.

**Sample Calculation:**

In case of maximum under-reinforced section with M40 grade of concrete, and Fe 500 steel-

$$\phi_{u,min} \times d = 0.07427 \text{ , } \phi_{y,min} \times d = 0.0024954$$

$$\mu_\phi = \frac{0.07427}{0.0024954} = 29.76$$

$$\theta_p = (0.07427 - 0.0024954) \times \frac{1}{2} = 0.035888 \text{ radians}$$

From the above observation, it may be stated that up to M60 grade of concrete, the curvature ductility of maximum under-reinforced section sincreases with higher concrete grades. However, beyond M60, the curvature ductility decreases as the grade of concrete increases. The results indicate that for the same grade of concrete, lower grades of steel exhibit higher curvature ductility values compared to higher grades of steel. The curvature ductility of sections as per IRC 112:2020[3], vary from 11.76 to 39.72. It has been reported that as per IS 456:2000[2] these values range from 6.09 to 23.44[1,6,27]. As per the guidelines of IS 13920:2016[7], curvature ductility of maximum under-reinforced sections will vary from 4.19 to 8.93[1,6,27].

#### *3.2.2 Evaluation of ductility and plastic rotations of balanced sections*

When a reinforced concrete section is in balanced condition, both the steel and concrete reach their limiting conditions at the same time, and the strain in steel will not increase beyond the yield strain. For balanced section, Stage-I (yield stage) is reached when the strain at outermost compression fibre in concrete reaches $_{c2}$ (as beyond this point stress in concrete remains constant with increase in strain) and Stage-II (ultimate stage) is reached when the limiting strain in concrete reaches $_{cu2}$, respectively.[1,38] The corresponding curvature ductility values and amount of plastic rotations have been calculated as discussed below.

3.2.2.1 Stage I - At yielding stage

According to the stress-strain diagram prescribed in IRC 112:2020[3], during Stage-I, the compressive strain in concrete reaches a value of $_{c2}$, and the parabolic

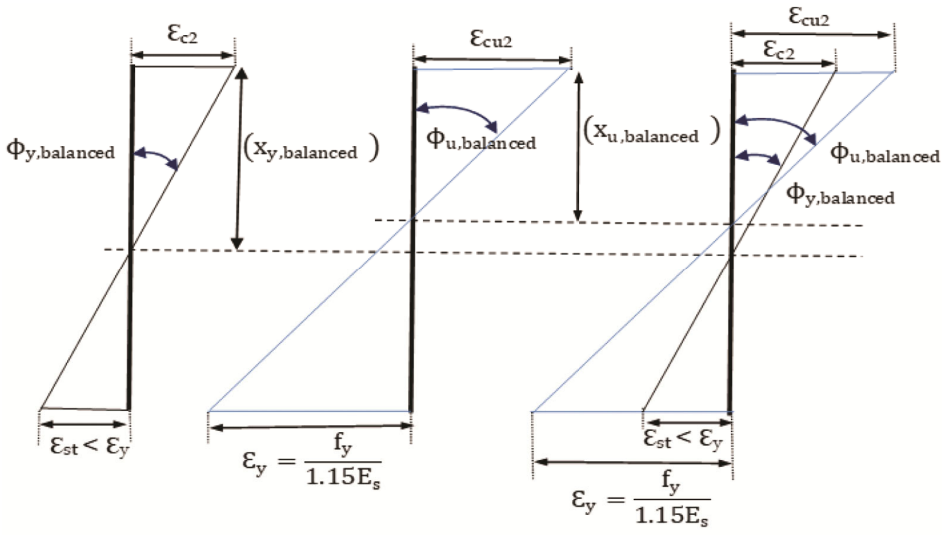


Fig. 8 — Strain Diagram for balanced section at yield and ultimate stages.

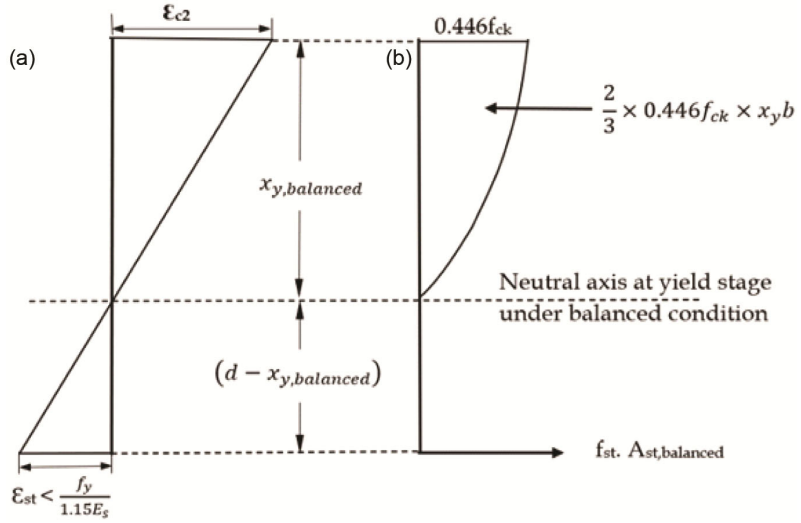


Fig. 9 — (a) Strain distribution diagram and (b) Stress block at Stage-I of balanced section.

portion of the stress block is formed only, as depicted in Figure 9. At this stage, it can be assumed that concrete is yielding, while steel has not yet reached the yield point. $x_{y,bal}$ is the depth of neutral axis in Stage-I in balanced condition as depicted in Figure 8.

From the strain distribution diagram, it can be stated that,

$$\frac{\varepsilon_{c2}}{x_{y,bal}} = \frac{\varepsilon_{st}}{(d - x_{y,bal})}$$

$$\text{or,} \quad \varepsilon_{st} = \frac{\varepsilon_{c2}}{x_{y,bal}}(d - x_{y,bal}) \qquad \ldots(16)$$

From force equilibrium equation as shown in Figure-9 it can be stated that,

$$\frac{2}{3} \times 0.446\, f_{ck} x_{y,bal} = f_{st} \times A_{st,\ balanced}$$

$$\text{or, } f_{st} = \frac{0.29733 f_{ck} x_{y,bal}}{A_{st,balanced}}$$

$$\text{or, } \varepsilon_{st} = \frac{0.29733 f_{ck} x_{y,bal}}{A_{st,balanced} \times E_s} \qquad \ldots(17)$$

Equating both the value of $\varepsilon_{st}$ from eqn.-16 and eqn.-17

$$0.29733.f_{ck}.\left(\frac{x_{y,bal}}{d}\right)^2 + \left(c2\, A_{st,balanced}.E_s\right)\left(\frac{x_{y,bal}}{d}\right) - \left(\varepsilon_{c2} \times A_{st,balanced} E_s\right) = 0 \qquad \ldots(18)$$

Table 10 — Depths of neutral axis and curvatures at yield stage in balanced section.

| Grades of concrete ($f_{ck}$) | Fe415/Fe415D/Fe415S | | Fe500/Fe500D/Fe500S | | Fe550/Fe550D | | Fe600 | |
|---|---|---|---|---|---|---|---|---|
| | $\frac{x_{y,bal}}{d}$ | $\phi_{y,bal} \times d$ | $\frac{x_{y,bal}}{d}$ | $\phi_{y,bal} \times d$ | $\frac{x_{y,bal}}{d}$ | $\phi_{y,bal} \times d$ | $\frac{x_{y,bal}}{d}$ | $\phi_{y,bal} \times d$ |
| M15 to M60 | 0.5971 | 0.00335 | 0.5536 | 0.00361 | 0.531 | 0.00377 | 0.5102 | 0.00392 |
| M65 | 0.5978 | 0.00351 | 0.5539 | 0.00379 | 0.531 | 0.00395 | 0.5100 | 0.00412 |
| M70 | 0.5965 | 0.00369 | 0.5521 | 0.00398 | 0.5291 | 0.00416 | 0.5079 | 0.00433 |
| M75 | 0.5935 | 0.00388 | 0.5486 | 0.00419 | 0.5253 | 0.00438 | 0.5039 | 0.00456 |
| M80 | 0.5889 | 0.00391 | 0.5438 | 0.00423 | 0.5204 | 0.00442 | 0.4989 | 0.00461 |
| M85 | 0.5884 | 0.00408 | 0.5430 | 0.00442 | 0.5194 | 0.00462 | 0.4978 | 0.00482 |
| M90 | 0.5829 | 0.00412 | 0.5373 | 0.00447 | 0.5137 | 0.00467 | 0.4920 | 0.00488 |

Table 11 — Ultimate depths of neutral axis and ultimate curvatures for balanced sections.

| Grades of concrete | Fe415/Fe415D/Fe415S | | Fe500/Fe500D/Fe500S | | Fe550/Fe550D | | Fe600 | |
|---|---|---|---|---|---|---|---|---|
| | $\frac{x_{u,bal}}{d}$ | $\phi_{u,bal} \times d$ | $\frac{x_{u,bal}}{d}$ | $\phi_{u,bal} \times d$ | $\frac{x_{u,bal}}{d}$ | $\phi_{u,bal} \times d$ | $\frac{x_{u,bal}}{d}$ | $\phi_{u,bal} \times d$ |
| M20 to M60 | 0.660 | 0.00531 | 0.617 | 0.00568 | 0.594 | 0.00589 | 0.573 | 0.00611 |
| 65 | 0.646 | 0.00511 | 0.603 | 0.00548 | 0.580 | 0.00569 | 0.558 | 0.00591 |
| 70 | 0.632 | 0.00491 | 0.588 | 0.00528 | 0.564 | 0.00549 | 0.543 | 0.00571 |
| 75 | 0.616 | 0.00471 | 0.571 | 0.00508 | 0.548 | 0.00529 | 0.526 | 0.00551 |
| 80 | 0.608 | 0.00461 | 0.563 | 0.00498 | 0.539 | 0.00519 | 0.518 | 0.00541 |
| 85 | 0.599 | 0.00451 | 0.554 | 0.00488 | 0.530 | 0.00509 | 0.508 | 0.00531 |
| 90 | 0.590 | 0.00441 | 0.545 | 0.00478 | 0.521 | 0.00499 | 0.499 | 0.00521 |

The depth of neutral axis factor, $\frac{x_{y,bal}}{d}$ can be determined for various grades of concrete by solving this quadratic equation. The results of this calculations are shown in Table 10. Curvature at Stage-I or yield curvature will be,

$$\phi_{y,balanced} = \frac{\varepsilon_{cy}}{(x_{y,bal})} = \frac{\varepsilon_{c2}}{\left(\frac{x_{y,bal}}{d}\right) \times d}$$

$$or, \phi_{y,balanced} \times d = \frac{\varepsilon_{c2}}{\left(\frac{x_{y,bal}}{d}\right)} \quad \ldots (19)$$

For all strengths of concrete ($\phi_{y,balanced} \times d$) values are presented in Table 10.

**Sample Calculation:**

In case of balanced section with M40 grade of concrete, and Fe 500 steel-

$\varepsilon_{c2} = 0.002$, $A_{st,balanced} = 0.02042$ (From Table 4)

by substituting in equation 18,

$$0.2973 \times 40\left(\frac{x_{y,bal}}{d}\right)^2 + (0.002 \times 0.02042 \times 2 \times 10^5)\left(\frac{x_{y,bal}}{d}\right) - (0.002 \times 0.02042 \times 2 \times 10^5) = 0$$

By solving this equation, $\frac{x_{y,bal}}{d} = 0.55363$

Hence, $\phi_{y,bal} \times d = \frac{\varepsilon_{c2}}{\left(\frac{x_{y,bal}}{d}\right)} = \frac{0.002}{0.55363} = 0.00361$

3.2.2.2 Stage II - At failure stage

At this stage, both the concrete and steel reach their respective limiting conditions. The section has attained its flexural strength and failure occurs due to the crushing of concrete, with the full stress block of concrete. However, the interval between Stage-I and Stage-II, caused by the increase in concrete strain from $\varepsilon_{c2}$ to $\varepsilon_{cu2}$ (as if due to yielding of concrete), is very small. As a result, yielding is minimal, leading to less curvature ductility values for balanced sections. The depth of the neutral axis at this stage is known as the balanced depth of neutral axis, $x_{u,bal}$, as shown in Figure 8. $\left(\frac{x_{u,bal}}{d}\right)$ has already been evaluated for all concrete strength classes and have been presented in Table 4. Curvature at this stage is ultimate curvature, $\phi_{u,balanced}$ can be calculated as-

$$\phi_{u,balanced} = \left(\frac{\varepsilon_{cu2}}{x_{u,bal}}\right)$$

$$\phi_{u,balanced} \times d = \left(\frac{\varepsilon_{cu2}}{\frac{x_{u,bal}}{d}}\right) \quad \ldots (20)$$

By using this $\left(\frac{x_{u,bal}}{d}\right)$, $\phi_u$ is calculated as per IRC 112:2020[3] and are presented in Table 11. Curvature ductility of a balanced section can be evaluated as described below.

Table 12 — Values of curvature ductility and plastic rotations for balanced sections.

| Grades of concrete | Curvature ductility and plastic rotations for balanced sections | | | | | | | |
|---|---|---|---|---|---|---|---|---|
| | Fe415/Fe415D/Fe415S | | Fe500/Fe500D/Fe500S | | Fe550/Fe550D | | Fe600 | |
| | Curvature Ductility ($\mu_\phi$) | Plastic rotations ($\theta_p$) (Radian) | Curvature Ductility($\mu_\phi$) | Plastic rotations ($\theta_p$) (Radian) | Curvature Ductility ($\mu_\phi$) | Plastic rotations ($\theta_p$) (Radian) | Curvature Ductility ($\mu_\phi$) | Plastic rotations ($\theta_p$) (Radian) |
| M20 to M60 | 1.584 | 0.00098 | 1.571 | 0.00103 | 1.564 | 0.00106 | 1.559 | 0.00110 |
| M65 | 1.453 | 0.00080 | 1.444 | 0.00084 | 1.440 | 0.00087 | 1.435 | 0.00090 |
| M70 | 1.330 | 0.00061 | 1.324 | 0.00065 | 1.321 | 0.00067 | 1.318 | 0.00069 |
| M75 | 1.214 | 0.00041 | 1.211 | 0.00044 | 1.209 | 0.00046 | 1.207 | 0.00047 |
| M80 | 1.179 | 0.00035 | 1.176 | 0.00037 | 1.175 | 0.00039 | 1.174 | 0.00040 |
| M85 | 1.104 | 0.00021 | 1.103 | 0.00023 | 1.102 | 0.00024 | 1.101 | 0.00024 |
| M90 | 1.07 | 0.00014 | 1.069 | 0.00015 | 1.069 | 0.00016 | 1.068 | 0.00017 |

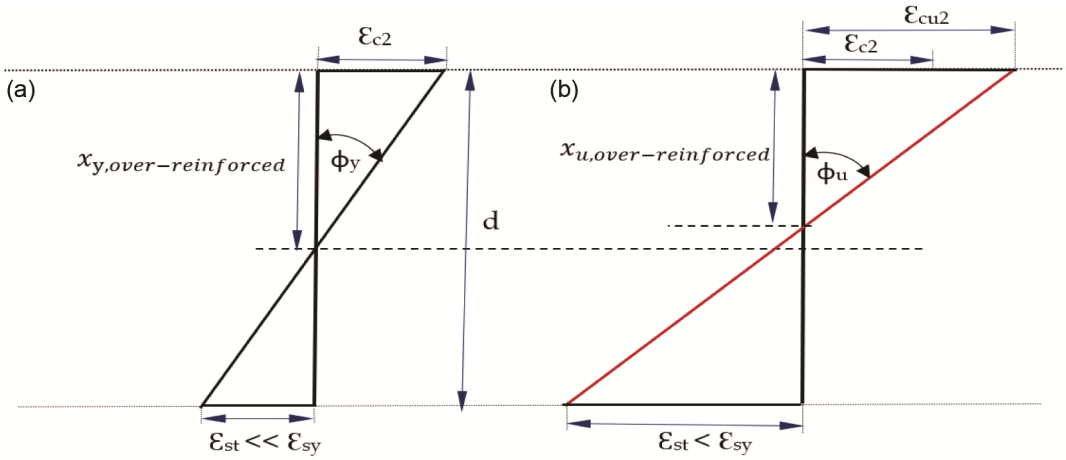


Fig. 10 — (a) Yield stage and (b) Ultimate stage at failure under over-reinforced condition.

$$\mu_{\phi,bal} = \frac{\phi_{u,bal}}{\phi_{y,bal}} = \frac{\phi_{u,bal} \times d}{\phi_{y,bal} \times d} \quad \ldots (21)$$

$$Plastic rotations, \theta_p = \left(\phi_{u,bal} - \phi_{y,bal}\right) \times \frac{d}{2}$$

$$\therefore \theta_p = \left(\phi_{u,bal} \times d\right) - \left(\phi_{y,bal} \times d\right) \times \frac{1}{2} \quad \ldots (22)$$

Curvature ductility values for balanced sections can be calculated in a manner similar to that of maximum under-reinforced section as discussed in the previous sections. Results are presented in Table 12. From the table, it has been observed that in a balanced section for a specific grade of steel, ductility values of balanced sections are same for M20 to M60 grades of concrete. This is because the limiting strains in concrete are constant for these concrete grades. However, for higher grades of concrete the ductility and plastic rotations decrease with increase in concrete grades. It is observed that curvature ductility of balanced sections decreases with increase in strength of steel.

#### *3.2.3 Evaluation of ductility and plastic rotations for maximum possible section condition based on $A_{st,max}$*

To calculate the curvature ductility and plastic rotations for sections with the maximum percentage of tension reinforcement, various methods are used depending on whether the sections are under-reinforced, balanced, or over-reinforced. The maximum possible condition of the section has already been defined in section 4.2. If the section lies within the under-reinforced region, the ductility values should be determined using the process explained in section 5.2.2. However, for sections in the over-reinforced region, the determination of curvature ductility and plastic rotations are presented below.

##### 3.2.3.1 Stage-I for over-reinforced condition

For over-reinforced condition, the Stage-I or yield stage is similar to that of the balanced condition as

Table 13 — Yield and Ultimate Curvatures for sections with maximum percentage of tension reinforcement as permitted by IRC 112.

| Ultimate and Yield Curvatures for maximum permitted sections | | | | | | | | | | | | |
|---|---|---|---|---|---|---|---|---|---|---|---|---|
| $f_{ck}$ | Fe415/Fe415D/Fe415S | | $f_{ck}$ | Fe500/Fe500D/Fe500S | | $f_{ck}$ | Fe550/Fe550D | | $f_{ck}$ | Fe 600 | |
| | $\Phi_{u,max}$ | $\Phi_{y,max}$ | | $\Phi_{u,max}$ | $\Phi_{y,max}$ | | $\Phi_{u,max}$ | $\Phi_{y,max}$ | | $\Phi_{u,max}$ | $\Phi_{y,max}$ |
| **Over-reinforced** | | | **Over-reinforced** | | | **Over-reinforced** | | | **Over-reinforced** | | |
| M20 | 0.00453 | 0.00279 | M20 | 0.00453 | 0.00279 | M20 | 0.00453 | 0.00279 | M20 | 0.00453 | 0.00279 |
| M25 | 0.00473 | 0.00293 | M25 | 0.00473 | 0.00293 | M25 | 0.00473 | 0.00293 | M25 | 0.00473 | 0.00293 |
| M30 | 0.00492 | 0.00307 | M30 | 0.00492 | 0.00307 | M30 | 0.00492 | 0.00307 | M30 | 0.00492 | 0.00307 |
| M35 | 0.00510 | 0.00320 | M35 | 0.00510 | 0.00320 | M35 | 0.00510 | 0.00320 | M35 | 0.00510 | 0.00320 |
| M40 | 0.00527 | 0.00332 | M40 | 0.00527 | 0.00332 | M40 | 0.00527 | 0.00332 | M40 | 0.00527 | 0.00332 |
| **Under-reinforced** | | | M45 | 0.00543 | 0.00344 | M45 | 0.00543 | 0.00344 | M45 | 0.00543 | 0.00344 |
| M45 | 0.00579 | 0.00315 | M50 | 0.00558 | 0.00355 | M50 | 0.00558 | 0.00355 | M50 | 0.00558 | 0.00355 |
| M50 | 0.00644 | 0.00313 | **Under-reinforced** | | | M55 | 0.00573 | 0.00365 | M55 | 0.00573 | 0.00365 |
| M55 | 0.00708 | 0.00310 | M55 | 0.00588 | 0.00374 | M60 | 0.00587 | 0.00375 | M60 | 0.00587 | 0.00375 |
| M60 | 0.00773 | 0.00308 | M60 | 0.00641 | 0.00371 | **Under-reinforced** | | | M65 | 0.00574 | 0.00398 |
| M65 | 0.00770 | 0.00306 | M65 | 0.00639 | 0.00369 | M65 | 0.00581 | 0.00406 | M70 | 0.00556 | 0.00421 |
| M70 | 0.00755 | 0.00306 | M70 | 0.00627 | 0.00369 | M70 | 0.00570 | 0.00406 | **Under-reinforced** | | |
| M75 | 0.00729 | 0.00304 | M75 | 0.00605 | 0.00366 | M75 | 0.00550 | 0.00403 | M75 | 0.00504 | 0.00440 |
| M80 | 0.00741 | 0.00302 | M80 | 0.00615 | 0.00364 | M80 | 0.00559 | 0.00400 | M80 | 0.00513 | 0.00437 |
| M85 | 0.00736 | 0.00302 | M85 | 0.00611 | 0.00364 | M85 | 0.00555 | 0.00400 | M85 | 0.00509 | 0.00437 |
| M90 | 0.00738 | 0.00300 | M90 | 0.00613 | 0.00362 | M90 | 0.00557 | 0.00398 | M90 | 0.00511 | 0.00434 |

shown in Figure 10 (a). Therefore, the expression for calculating the depth of neutral axis in the yield stage, i.e., $\left(\frac{x_{y,or}}{d}\right)$, will be the same as that expressed in the Stage-I in balanced condition and can be calculated from equation 18 by incorporating maximum percentage of steel as $A_{st}$. Correspondingly, the curvatures at the yield stage $(\phi_{y,or})$ for over-reinforced condition will be equal to $\frac{\varepsilon_{c2}}{\left(\frac{x_{y,or}}{d}\right)}$. This has been calculated and presented in Table 13 up to the grade of concrete where over-reinforced section is permitted.

3.2.3.2 Stage-II for over-reinforced condition

At the ultimate stage for over-reinforced sections, the concrete strain reaches $_{cu2}$and the steel strain $(\varepsilon_{st})$ is less than the yield strain in steel, $\frac{f_y}{1.15E_s}$. This has been shown in figure 10(b). According to IRC 112[3], the maximum percentage of steel and corresponding depth of neutral axis have been determined and presented in Table 5. Over-reinforced sections should be designed for specific concrete and steel grades where the maximum percentage of tension reinforcement is higher than the balanced percentage, as indicated in Table 5. At this stage, the corresponding maximum depth of the neutral axis factor is denoted by $\frac{x_{u,or}}{d}$ and the curvature can be calculated as the ratio of $_{cu2}$ and$x_{u,or}$.

$$\phi_{u,or} = \frac{cu2}{(x_{u,or})}$$

$$\therefore \phi_{u,or} \times d = \frac{cu2}{\left(\frac{x_{u,or}}{d}\right)} \quad \ldots (23)$$

The values are presented in Table 13.

Curvature ductility for the maximum permitted sections will be as follows.

$$\mu_\phi = \frac{\phi_{u,or}}{\phi_{y,or}}. \quad \ldots (24)$$

Plastic Rotation,

$$\theta_p = \phi_p \times l_p = (\phi_{u,or} - \phi_{y,or}) \times \frac{d}{2} \quad \ldots (25)$$

The values of curvature ductility and plastic rotations for sections with maximum percentage of tension reinforcement as per IRC 112:2020 have been presented in Table 14.

The ductility values of these sections are less compared to balanced and under-reinforced sections. It has been observed that for cases where sections with maximum percentage of tension reinforcement lies in over-reinforced region, ductility values increase with increase in grades of concrete but when the sections become under-reinforced, ductility values decrease with increase in grades of concrete. On the other hand, for all cases ductility values decrease with increase in grades of steel.

Table 14 — Plastic rotations and curvature ductility for section with maximum percentage of tension reinforcement as permitted in IRC 112.

| Curvature ductility and plastic rotations for maximum permitted sections | | | | | | | | | | | | |
|---|---|---|---|---|---|---|---|---|---|---|---|---|
| | Fe 415 | | | Fe 500 | | | Fe 550 | | | Fe 600 | | |
| $f_{ck}$ | $(\mu_\phi)$ | $\Theta_p \times d$ | $f_{ck}$ | $(\mu_\phi)$ | $\Theta_p \times d$ | $f_{ck}$ | $(\mu_\phi)$ | $\Theta_p \times d$ | $f_{ck}$ | $(\mu_\phi)$ | $\Theta_p \times d$ |
| **Over-reinforced** | | | **Over-reinforced** | | | **Over-reinforced** | | | **Over-reinforced** | | |
| M20 | 1.624 | 0.00059 | M20 | 1.624 | 0.000457 | M20 | 1.624 | 0.000380 | M20 | 1.624 | 0.000303 |
| M25 | 1.611 | 0.00069 | M25 | 1.611 | 0.000558 | M25 | 1.611 | 0.000481 | M25 | 1.611 | 0.000404 |
| M30 | 1.601 | 0.00078 | M30 | 1.601 | 0.000652 | M30 | 1.601 | 0.000575 | M30 | 1.601 | 0.000499 |
| M35 | 1.593 | 0.00087 | M35 | 1.593 | 0.000741 | M35 | 1.593 | 0.000664 | M35 | 1.593 | 0.000588 |
| M40 | 1.585 | 0.00096 | M40 | 1.585 | 0.000826 | M40 | 1.585 | 0.000749 | M40 | 1.585 | 0.000673 |
| **Under-reinforced** | | | M45 | 1.502 | 0.001814 | 1.579 | 1.441 | 0.000830 | 1.579 | 1.384 | 0.000753 |
| M45 | 1.838 | 0.001321 | M50 | 1.574 | 0.000984 | M50 | 1.574 | 0.000907 | M50 | 1.574 | 0.000831 |
| M50 | 2.059 | 0.001656 | **Under-reinforced** | | | M55 | 1.522 | 0.000982 | 1.569 | 1.461 | 0.000905 |
| M55 | 2.282 | 0.001989 | M55 | 1.572 | 0.00106 | M60 | 1.565 | 0.001053 | M60 | 1.565 | 0.000977 |
| M60 | 2.507 | 0.002322 | M60 | 1.727 | 0.00134 | **Under-reinforced** | | | M65 | 1.313 | 0.001279 |
| M65 | 2.517 | 0.002321 | M65 | 1.734 | 0.00135 | M65 | 1.433 | 0.000878 | M70 | 1.321 | 0.000612 |
| M70 | 2.467 | 0.002245 | M70 | 1.700 | 0.00129 | M70 | 1.405 | 0.000820 | **Under-reinforced** | | |
| M75 | 2.399 | 0.002126 | M75 | 1.653 | 0.00119 | M75 | 1.366 | 0.000736 | M75 | 1.148 | 0.00032 |
| M80 | 2.454 | 0.002197 | M80 | 1.691 | 0.00125 | M80 | 1.397 | 0.000795 | M80 | 1.174 | 0.00038 |
| M85 | 2.437 | 0.00217 | M85 | 1.679 | 0.00123 | M85 | 1.387 | 0.000775 | M85 | 1.166 | 0.00036 |
| M90 | 2.460 | 0.002191 | M90 | 1.694 | 0.00125 | M90 | 1.4 | 0.000796 | M90 | 1.177 | 0.00038 |

***3.2.4 Desirable values of ductility as per previous research work***

Different researchers have proposed different values of ductility. Matejčeková *et al*. proposed that earthquake-resistant structures should be built with structural steel that has strain ductility values of at least 15[39]. According to Dowrick, the desirable curvature ductility values ($\mu_\varphi$) for reinforced concrete beam sections during seismic activity should be between 10 and 20[38].Different researchers have suggested that the minimum value of curvature ductility ($\mu_{\varphi,\min}$) should be 3.32 for non-earthquake resistant structures and higher for earthquake-resistant structures[41,15,42,43] A curvature ductility factor of at least 10 is preferable in seismic design [14]. It has been reported that in a well-designed frame structure, the curvature ductility of the section should always be greater than 4μ, where μ is the displacement ductility factor that ranges from 3 to 5. Therefore, the minimum curvature ductility for a well-designed structure should range between 12 and 20[26,44]. According to Paulay and Priestley, a minimum curvature ductility factor of 8 is considered sufficient for moderate earthquakes[24,38]. Another reference suggests that a minimum curvature ductility factor of 5 is adequate for any structure[45].The ductility values as per IS 456:2000[2] and IS 13920:2016[6] have been reported in a number of publications[1,6,25]. In Table 15 the ductility and plastic rotations of beam sections as per IS 456:2000[2], IS 13920:2016[7] and IRC 112:2020[3] are presented in detail.The minimum desirable value of curvature ductility has been reported as 3.32 as mentioned above. Evaluating the curvature ductility values as per different Indian standards, as mentioned in Table 15, it can be concluded that the maximum curvature ductility of balanced section is 1.89, which is much less than the desired value. Hence balanced sections or sections close to balanced conditions do not qualify for the desirable ductility values and designers should always opt for sections which are significantly under-reinforced. The maximum curvature ductility value for a section with minimum percentage of tension reinforcement is 39.27, which is very high but it will result in significant amount of plastic rotation of the section and can surpass higher performance-based limit state conditions causing serious damage to the section. Hence maximum

Table 15 — Ductility and plastic rotation values as per different Indian standards.

| As per different standards | Strain Ductility of Maximum under-reinforced sections | Curvature ductility | | | Plastic Rotations (Radians) | | |
|---|---|---|---|---|---|---|---|
| | | Maximum under-reinforced sections | Balanced section | Sections with Maximum percentage of tension reinforcement | Maximum under-reinforced sections | Balanced section | Sections with Maximum percentage of tension reinforcement |
| As per IS 456:2000 | 6.62 – 25.98[27] | 6.09 to 23.44[1,6] | 1.87 to 1.98[1,6] | Over-reinforced not allowed | 0.0142 to 0.0489[1,6] | 0.00171 to 0.00186[1,6] | Over-reinforced not allowed |
| As per IS 13920:2016 | 4.51 - 10.12[27] | 4.19 to 8.93[1,6] | | | 0.0096 to 0.0187[1,6] | | |
| As per IRC 112:2020 (Present Study) | 12.89 – 44.35 | 12.45 to 39.27 | 1.07 to 1.56 | 1.15 to 1.57 | 0.017076 to 0.040713 | 0.0011 to 0.00098 | 0.00038 to 0.00219 |

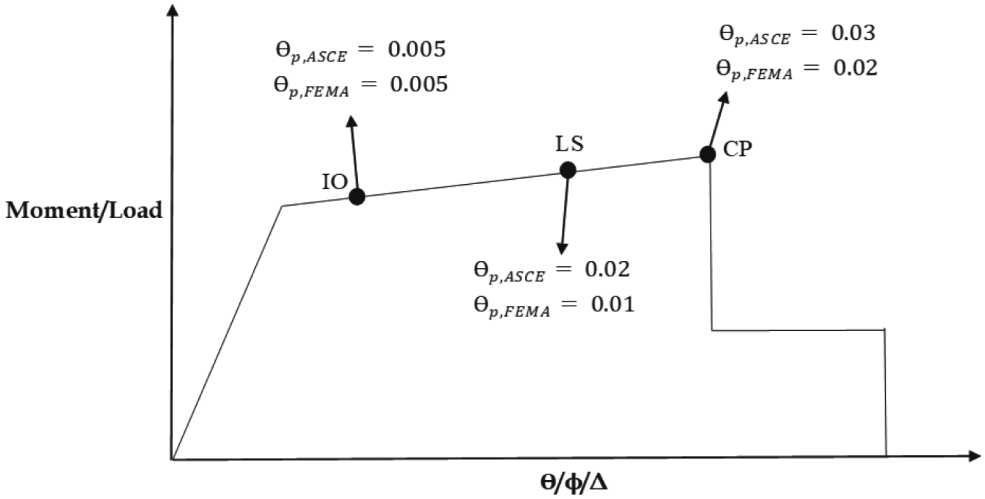


Fig. 11 — Different performance-based limit states as per international guidelines and standards[29,46].

under-reinforced sections are also not at all preferred. From the above study it transpires that along with strength and serviceability design some form of quantification of ductility values can optimize section design significantly.

### 3.3 Damage assessment of section corresponding to different performance levels of PBD

International guidelines and standard like FEMA 356[31], ATC 40[30] and ASCE 41-13[46]specify different plastic rotation values with reference to acceptance criteria at Immediate Occupancy (IO), Life Safety (LS) and Collapse Prevention (CP) performance levels as presented in Figure 11. For conservative design the highest prescribed values have been considered and compared with the calculated ones. ASCE41-13[46] presents plastic rotation angle (radians) limits for IO, LS and CP levelsas 0.005, 0.02 and 0.03 respectively in case of reinforced concrete beam. In contrast FEMA 356 and ATC 40 recommend plastic rotation angles for section in flexure as 0.005, 0.01, and 0.02 for IO, LS and CP level respectively. These are clearly depicted in Figure 11.

By comparing the plastic rotation values obtained in the present study with thoseprescribed in FEMA 356. ATC 40, and ASCE 41-13, the performance of the sections and the associated damage level can be assessed. The present study has shown that the maximum under-reinforced sections according to IRC 112[3] possess plastic rotations ranging from 0.0107 to 0.0407. These values are significantly higher than the values recommended for different performance levels in performance-based design. When comparing the values in Table 10 with the performance levels in performance-based design as per FEMA 356, it can be concluded that all maximum under-reinforced sections have plastic rotations exceeding the Collapse Prevention (CP) level i.e., 0.02 radian. As per ASCE 41-13, only few cases like with Fe 415, M20, with Fe 500 up to M25, and with Fe550 and Fe 600 grade steel up to M30 grade concrete section lies within the CP

level but for all other cases the values are higher than the CP level. Hence it can be inferred that these sections will cross the collapse prevention stage. The minimum percentage of tension reinforcement as specified in IRC 112[3] needs to be revised to avoid such damage levels. In this context it may be mentioned that the minimum percentage of tension reinforcement in beams is generally provided with respect to cracking moment consideration. The present study indicates that along with cracking moments of resistance, performance-based limit state condition should be considered in arriving at the minimum percentage of tension reinforcement in beams. Based on the results of the present study, it is recommended that significant modifications in the prescribed minimum area of tension reinforcement in beams are necessary to avoid the section reaching collapse prevention stage. On the other hand, the plastic rotation values for balanced and maximum permitted sections, presented in tables 12 and 13 respectively, are much lower and fall within the Immediate Occupancy (IO) level.

## 4 Conclusion

IS 456, which is the mother code of concrete in India is more than 24-year-old and is significantly lagging in the field of new generation material properties and design philosophy. IRC 112, code on concrete road bridges has been recently revised and the reinforced concrete design provisions are in line with international standards like Eurocode-2 (2004). In the present work, to cope with the present day reinforced concrete design philosophy and material properties, the reinforced concrete design provisions relating to ductility, which is a very important virtue for earthquake resistance structures have been explored in detail. It is expected that the forthcoming revision of IS456 will have similar design provisions. The validity of the limit state methods ends at the limiting or the design loads but during earthquakes structures can be forced to go beyond the limit states and hence ductility plays vital role in conservation of life and property under such circumstances. However, in our day-to-day design ductility is not given the desired level of importance and the present study is a humble effort to highlight the contribution of ductility in the design of flexural members.

From the present work following conclusions may be drawn -

a It can be inferred that the IRC 112-2020, though permits all types of section failure, allows over-reinforced section design only for the following conditions –

(i) with HYSD steel grade Fe415/Fe415S/Fe415D up to M40 concrete (ii) with HYSD steel grade Fe500/Fe500S/Fe500D up to M50 concrete (iii) with HYSD steel grade Fe500/Fe500D up to M60 concrete and (iv) with HYSD steel grade Fe600 up to M70 grade of concrete.

b According to IRC 112:2020, the strain ductility values for sections with minimum area of tension reinforcement fall within the range of 15.732 to 40.314. The strain ductility is inversely proportional to the strength of steel. On the other hand, for concrete grades up to M60, strain ductility increases with increase in concrete strength. However, beyond M60, the strain ductility tends to decrease as the strength of concrete increases.

c It has been observed that for a constant grade of steel, section ductility of maximum under-reinforced section sincreases with an increase in grade of concrete up to $M60$ and thereafter the values decrease gradually up to M90 grade of concrete. Hence M60 grade of concrete can be considered as optimum from the requirement of ductility. However, the present study suggests that for a constant grade of concrete, lower grades of steel possess higher curvature ductility values compared to higher grades of steel. It can also be inferred that Fe 415 grade of steel results in optimum design from the consideration of ductility.

d The results indicate that under balanced condition, the ductility values remain constant across M20 to M60 grades of concrete for a specific grade of steel. This consistency arises since the limiting strain in concrete remains constant for these concrete grades. Beyond M60, ductility values get reduced.

e It has already been established that under-reinforced sections consistently exhibit improved performance in terms of ductility compared to balanced or over-reinforced sections. As the degree of under-reinforcement increases, the level of ductility also increases, accompanied by greater plastic rotations. Consequently, it can be concluded that for the design of structures in seismic zones, under-reinforced sections are always preferred over balanced or over-reinforced sections.

f Sections with minimum percentage of tension reinforcement specified by IRC 112:2020 exhibit exceptionally high levels of ductility and are associated with significantly high plastic rotations.

The calculated plastic rotation values often surpass the limiting plastic rotation value as prescribed for the collapse prevention stage of Performance Based Design (PBD). Therefore, the section conditions may extend beyond the Collapse Prevention (CP) stage of PBD, resulting in considerable risks to life and property.

g The minimum percentage of tension reinforcements in beams is typically determined based on the cracking moment of resistance of the sections. However, since the associated plastic rotations are excessively high, the sections can fail due to damage resulting from these deformation levels, which can be assessed using the specifications of PBD. This represents a drawback of IRC 112:2020, and it is necessary to revise the requirements for the minimum area of tension reinforcement in beams to ensure that the plastic rotations remain within an acceptable safety level.

## Acknowledgements

We would like to acknowledge that the authors did not receive any financial assistance or support for this work. All the authors have made similar contributions to the work.

## References

1 Jha B & Bhanja S, *Asian J Civil Eng*, 22(4) (2021) 769.
2 IS 456:2000, Plain and Reinforced Concrete – Code of Practice, Bureau of Indian Standards (New Delhi), 2000, 100 pp.
3 IRC 112:2020, Code of Practice for Concrete Road Bridges, Indian Roads Congress (New Delhi), 2020.
4 EN 1992-1-1:2004, Eurocode 2: Design of Concrete Structures – Part 1-1: General Rules and Rules for Buildings, CEN (Brussels), 2004.
5 Mandal A & Bhanja S, *Indian Concrete J*, 98(8) (2024) 1.
6 Bhanja S, **Reinforced Concrete Design: Limit State Method and Beyond**, (CRC Press,Taylor & Francis Group, Boca Raton, USA), ISBN: 9781032458892, 2024.
7 IS 13920:2016, Ductile Design and Detailing of Reinforced Concrete Structures Subjected to Seismic Forces, Bureau of Indian Standards (New Delhi), 2016, 16 pp.
8 Mandal B, Jha B K & Bhanja S, *Indian Concrete J,* 98(10) (2024) 40.
9 Bhatt P, MacGinley T J & Choo B S, **Reinforced Concrete: Design Theory and Examples**, (CRC Press, Boca Raton, USA), ISBN: 13: 978-0-415-30796-3, 2005. p424-430
10 Bouzid H & Kassoul A, *Struct Eng Mech,* 58(1) (2016) 1.
11 Arslan M H, *KSCE J Civil Eng,* 16 (2012) 759.
12 Lopes A V, Lou T & Lopes S M, *Eng Struct,* 322 (2025) 119105.
13 Xie Y, Ahmad S H, Yu T, Hino S & Chung W, *ACI Struct J,* 91(2) (1994) 140.
14 Kwan A K H & Ho J C M, *Adv Struct Eng,* 13(4) (2010) 651.
15 Park R & Ruitong D, *ACI Struct J,* 85(2) (1988) 217.
16 Alghazawi O K, *Civil Eng Archit,* 11(2) (2023) 847.
17 Mondal P, Samanta A K & Roy D K S, *Mater Today Proc* (2023).
18 Laterza M, D'Amato M, Thanthirige L P, Braga F & Gigliotti R, *Open Constr Build Technol* J, 8(1) (2010) 132.
19 Arslan G & Cihanli E, *J Civil Eng Manag,* 16(4) (2010) 462.
20 Opabola E A & Elwood K J, J *Struct Eng*, 149(4) (2023) 04023020.
21 Lopes S M R & Bernardo L F A, *Mater Struct,* 36 (2003) 22.
22 Foroughi S & Yuksel S B, *Slovak J Civil Eng,* 30(1) (2022) 8.
23 Paulay T & Priestley M J N, **Seismic Design of Reinforced Concrete and Masonry Buildings**, John Wiley & Sons (New York), 1992.
24 Medhekar M S & Jain S K, *Bridge & Struct Eng*, XXIII(2) (1993) 78.
25 Park R & Paulay T, *Bull N Z Natl Soc Earthq Eng,* 8(1) (1975) 1.
26 Jha B K & Bhanja S, *Indian Concrete J,* 96(10) (2022) 1.
27 Shah V L & Karve S R, **Limit State Theory and Design of Reinforced Concrete,**(Structures Publications, Pune), ISBN: 978-8190371711,2016.
28 Kara I F, Ashour A F & Dundar C, *Struct Eng Mech,* 63(5) (2017) 669.
29 ATC-40, Seismic Evaluation and Retrofit of Concrete Buildings, Vol. 1, Applied Technology Council (California), 1996.
30 FEMA 356, Prestandard and Commentary for the Seismic Rehabilitation of Buildings, Federal Emergency Management Agency (Washington D.C.), 2000.
31 López-López A, Tomás A & Sánchez-Olivares G, *Eng Struct,* 124 (2016) 245.
32 Shen X, Li B, Chen Y T, Tizani W & Jiang Y, *Eng Struct,* 251 (2022) 113468.
33 Pokhrel M & Bandelt M J, *Eng Struct,* 200 (2019) 109699.
34 Park R & Paulay T, **Reinforced Concrete Structures**, (John Wiley & Sons, New York), ISBN: 978-81-265-2382-5, 1975.
35 Hillerborg A, *Eng Fract Mech,* 35 (1990) 233.
36 Carpinteri A & Corrado M, *Eng Fract Mech,* 77(7) (2010) 1091.
37 Priestley M J N, Calvi G M & Kowalsky M, **Displacement-Based Seismic Design of Structures**, (IUSS Press, Pavia, Italy), ISBN:978-8861980006, 2007.
38 Matejčeková-Farhat M & Ároch R, *Slovak J Civil Eng,* 21(3) (2013) 1.
39 Dowrick D J, **Earthquake Resistant Design,** (John Wiley & Sons, Chichester, UK), ISBN: 0471915033, 1987.
40 Kwan A K H, Au F T K & Chau S L, *Mag Concr Res,* 56(5) (2004) 299.
41 Lam J Y K, Ho J C M & Kwan A K H, *Comput Concr,* 6(5) (2009) 357.
42 Au F T K & Kwan A K H, *Comput Concr,* 1(2) (2004) 115.
43 Park R, *Proc 6th World Conf Earthq Eng,* (New Delhi), 1977.
44 Pillai S U & Menon D, **Reinforced Concrete Design**, (Tata McGraw Hill Education Pvt Ltd, New Delhi), 3rdEdn, ISBN: 13-978-0070141100, 2012.
45 ASCE/SEI 41-13, Seismic Evaluation and Retrofit of Existing Buildings, American Society of Civil Engineers (Reston, Virginia), 2014.